



## Testing and reopening in an SEIR model <sup>☆</sup>

David Berger <sup>a,1</sup>, Kyle Herkenhoff <sup>b,c,2</sup>, Chengdai Huang <sup>d</sup>, Simon Mongey <sup>d,3</sup>

<sup>a</sup> Duke University, United States of America

<sup>b</sup> Federal Reserve Bank of Minneapolis, United States of America

<sup>c</sup> University of Minnesota, United States of America

<sup>d</sup> Kenneth C. Griffin Department of Economics, University of Chicago, United States of America



### ARTICLE INFO

#### Article history:

Received 29 April 2020

Received in revised form 28 October 2020

Available online 27 November 2020

#### Keywords:

COVID-19

Virological testing

Serological testing

Reopening

Quarantine

### ABSTRACT

We quantify how testing and targeted quarantine make it possible to reopen an economy in such a way that output increases while deaths are reduced. We augment a standard Susceptible-Exposed-Infectious-Recovered (SEIR) model with (i) virological testing, (ii) serological testing, (iii) permanently asymptomatic individuals, (iv) incomplete information, and (v) a reduced form behavioral response of reopening to changes in health risks. Virological testing allows for targeted quarantine of asymptomatic spreaders. Serological testing allows for targeted release of recovered individuals. We fit our model to U.S. data. Virological tests every two weeks accommodate more aggressive reopening that more than halves output losses while keeping deaths below forecasts under the status quo. Serological tests are much less effective. Implementing testing against a fixed budget, low sensitivity tests that are cheap and used frequently, dominate perfect tests that are expensive and used less frequently.

© 2020 Elsevier Inc. All rights reserved.

“Once again, our key message is: test, test, test.” – World Health Organization (Twitter), March 16, 2020

## 0. Introduction

During a pandemic, testing can accommodate targeted lockdown policies and in doing so allow for broad reopening policies that support economic output. We show this and quantify public health and economic outcomes by augmenting a standard epidemiological model with (i) virological testing, (ii) serological testing, (iii) temporarily and permanently asymptomatic individuals, and (iv) behavior that responds to public health outcomes. These are important for understanding the response to COVID-19 given three facts.<sup>4</sup> First, there is a high rate of permanently asymptomatic infection. Second, individuals that develop symptoms are highly infectious in their pre-symptomatic stages. Third, depression of disease transmission rates across U.S. states absent large scale testing regimes has been well documented (Atkeson et al., 2020).

<sup>☆</sup> We thank David Dam and Meghana Gaur for excellent research assistance. The views expressed in this study are those of the author and do not necessarily reflect the position of the Federal Reserve Bank of Minneapolis or the Federal Reserve System.

E-mail addresses: [kyle.herkenhoff@gmail.com](mailto:kyle.herkenhoff@gmail.com) (K. Herkenhoff), [mongey@uchicago.edu](mailto:mongey@uchicago.edu) (S. Mongey).

<sup>1</sup> <https://sites.google.com/site/davidwberger>.

<sup>2</sup> <https://sites.google.com/site/kyleherkenhoff/>.

<sup>3</sup> <http://www.simonmongey.com>.

<sup>4</sup> As of August 2020 these have been documented in a number of peer-reviewed publications, e.g. see the meta-analysis of peer-reviewed and unpublished papers in Byambasuren et al. (2020).

The two types of asymptomatic imply a role for both virological and serological tests. Once infected, both permanent and temporary asymptomatic types are unaware they are infectious. Virological testing of those without symptoms identifies these types and makes targeted quarantine possible. Mortality and disease transmission fall, creating room to reduce quarantine measures, which we refer to as *reopening*. This mitigates the decline in output. Recovered types that never developed symptoms are unaware of their recovery. Serological testing of those without symptoms identifies these types and makes possible targeted release. Output increases, and disease transmission falls as recovered types crowd out interactions between susceptible and infected types, leading to fewer deaths. Which test provides better health and economic outcomes is an important quantitative question that we answer.

To quantify these mechanisms, we include the minimal necessary modifications to a standard epidemiological model. Fig. 1 provides a model schematic. We start with the SEIR model which has four states: Susceptible (S), Exposed (E), Infected (I) and Recovered (R). First, we split the exposed state into two groups: those who are temporarily asymptomatic and those who are permanently asymptomatic, where only temporary asymptomatic cases develop symptoms before recovery or death. Second, we assume both types spread the disease.<sup>5</sup> Third, we introduce incomplete information. Asymptomatic individuals do not know their own health state, nor does the planner. This creates a role for virological tests. Fourth, our two types of infection generate two types of recovered individuals: known recovered and unknown recovered. Incomplete information implies that unknown recovered and susceptible types cannot be distinguished. This creates a role for serological tests. Fifth, we assume that individuals exit quarantine in a way that depends on both (i) the level of deaths in the economy and (ii) government policy (e.g. reopening parks, gyms, etc.). We refer to the component of the quarantine exit rate determined by the government as ‘reopening’ policy. The endogenous component of the quarantine exit rate allows us to match time-series data on deaths and reproduction numbers and is consistent with theory (Farboodi et al., 2020).

We calibrate the model in order to construct counterfactual time-series for health outcomes and economic output. We assume that economic output is proportional to the number of healthy non-quarantined individuals. We adopt as many agreed-upon medical parameters from the literature as possible and calibrate the remaining model parameters. Since many parameters are unknown we conduct extensive robustness exercises. In our calibration we take as given the shutdown of the US economy over March and April 2020, and choose the rate of disease transmission and effectiveness of the shutdown to match the time-series of deaths between March and June. We then allow individuals to respond to changes in deaths by emerging out of quarantine so long as deaths stay depressed. This death-dependent exit rate from quarantine is calibrated to match mortality in July and August.

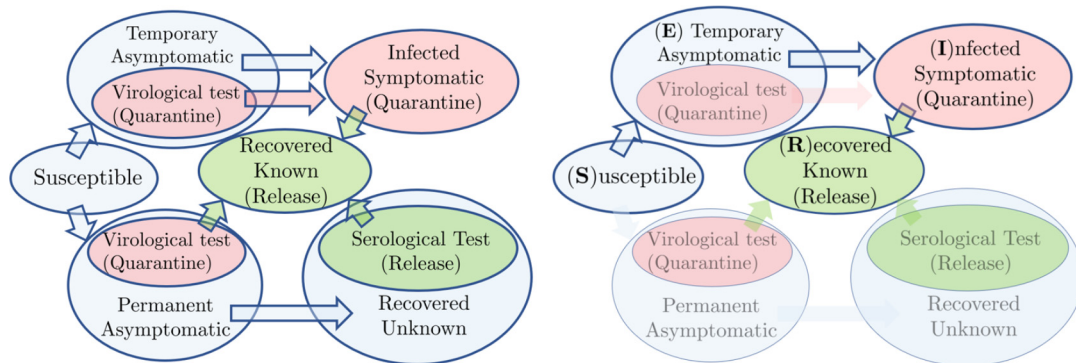
Our main counterfactual answers the question: “If testing is increased, how much can the economy be additionally reopened while minimizing the loss of lives?”. Testing saves lives as it comes coupled with targeted quarantine (release) measures in the case of virological (serological testing). In our calibrated benchmark with only the endogenous component of reopening, we forecast total deaths under the pandemic:  $D$ . In counterfactual economies with testing at frequencies that range from one to 12 weeks, we then compute the permissible additional reopening such that deaths do not exceed  $D$ . We then compare the benchmark and counterfactual economies in terms of the profile of infections and output losses.

Our main result is that by combining increased testing with targeted quarantine, it is possible to reopen the economy and produce significantly more while not exceeding the cumulative deaths the US is currently on track to incur. First, if virological tests are administered to individuals on average every two weeks, then 53 percent of the output lost under the no testing case can be saved. Even with monthly testing 20 percent of lost output is recovered. Second, we find that serological testing has quantitatively minor effects relative to virological tests, an important result for the selection of testing regimes. Simply put, with fewer than 16 percent of people ever becoming infected in the benchmark, there is little scope to improve output losses by identifying these individuals. We provide a range of robustness analysis. In particular we make the best case for serological testing by making the identification of antibodies necessary before release from quarantine, irrespective of past symptoms or virological tests. Even in this setting, serological tests have small effects.

Our third main result is to quantify the trade-off between test quality and frequency that a government may face when implementing a virological testing regime. Non-linearities in the model imply that frequency may be more important than quality. We consider two tests: (i) an at-home test that costs \$10 with a 50 percent false negative rate, and (ii) an accurate lab test (Polymerase Chain Reaction or ‘PCR’ tests) that costs \$40 with a zero false negative rate. For a fixed testing budget, at home testing can be done more frequently. Despite significantly lower accuracy, frequent at-home tests dominate the more accurate, expensive and infrequent PCR tests. Relative to PCR tests under a budget of \$40 per person per month, at-home tests save over 130,000 lives. As a consequence of saving more lives, people exit quarantine at a higher rate and output declines by around 9 percent less.

We conclude with a discussion of how policies in the model differ from the US experience. We feature random testing of asymptomatic individuals at high frequencies. The US experience has been to mainly test symptomatic individuals. We provide data on testing rates and programs at private institutions—e.g. college campuses—which are entirely consistent with our model. We discuss potential reasons the US policy deviates so much from that of private institutions.

<sup>5</sup> In the textbook SEIR model, exposed (E) types do not spread the disease and play very little role other than slowing down disease dynamics.



Notes: Blue states are unknown to the planner and individual. Red states are known positive and green states are known negative. Virological (serological) testing takes unknown individuals and transits them to the known positive (known negative) states. On the right, testing and permanent asymptomatic infection are shut-down, yielding the standard SEIR model.

Fig. 1. Model schematic (left), and the nested SEIR model (right). (For interpretation of the colors in the figure(s), the reader is referred to the web version of this article.)

Our exercises qualitatively and quantitatively contribute an important point for economists integrating epidemiological and macroeconomic models. Analysis of an economic model with an epidemiological block but without public health interventions such as testing and targeted quarantine unavoidably feature a trade-off between mortality and economic activity: faster reopening increases output but increases mortality. Kaplan et al. (2020) label the set of such outcomes a ‘pandemic possibility frontier’. Combining widely advocated public health measures of testing and targeted quarantine, our model delivers lower mortality and higher economic activity, significantly shifting this frontier outwards. Theories of economic-activity vs. mortality trade-offs with only a lock-down policy available to the policy-maker are hence necessarily discussions of second best policies.

This paper has eight sections. Section 1 reviews the related SEIR literature and recent papers using this model to quantify the effects of the coronavirus pandemic. Section 2 reviews data on infection, mortality, testing and quarantine measures. Section 3 describes the model. Section 4 details calibration and model fit. Section 5 provides our main counterfactuals which compute output savings delivered from a combination of elevated testing and targeted reopening. Section 6 considers the quality-frequency trade-off. Section 7 shows how our results are robust to many assumptions regarding the virus. Section 8 compares the testing policy in the paper to that observed on college campuses in August, 2020. Section 9 concludes. An appendix contains details on additional robustness exercises.

### 1. Literature

Brauer and Castillo-Chavez (2012) provide a summary of recent SEIR models. SEIR stands for Susceptible, Exposed (people not yet infectious in the standard model), Infectious, and Removed (quarantined or immune). In particular, they discuss frameworks of quarantine (setting aside individuals who are exposed) and isolation (setting aside individuals who are infectious, often called hospitalization).

A recent policy paper by Imperial College COVID-19 Response Team (2020) incorporates several policy parameters into an SEIR model that is enriched to accommodate geographical transmission and age dependency of transmission and mortality rates. In particular, they consider a model with quarantine, asymptomatic patients, and testing of hospitalized patients, with policy thresholds that depend on positive test rates. Their predictions have been reported widely in the press, and the model is being updated in real-time as this article is written. To the best of our knowledge, our contribution is to model (i) the matching process between different subgroups, thus endogenizing  $R_0$ , (ii) highlighting the importance of testing asymptomatic patients and, (iii) quarantine policies that are contingent on the testing outcomes. Lastly, we use our measure of the fraction of individuals quarantined as a measure of loss of economic activity. This allows us to evaluate the role of widespread testing which, as a policy, may allow for similar mortality rates but lower quarantine rates.

Recent examples of testing and diagnosis in an SEIR model include Chowell et al. (2003) who model the Severe Acute Respiratory Syndrome (SARS) epidemic in 2002. The purpose of testing and diagnosis in Chowell et al. (2003) is an improvement in healthcare, which reduces the time to recovery by one half.<sup>6</sup> In our model, the role for testing and diagnosis is being able to efficiently target quarantine measures.

Recent examples of quarantine in an SEIR model include Feng (2007) who derives closed form expressions for the maximum and final rates of infection. Feng (2007) has two notions of quarantine: one in which exposed individuals are

<sup>6</sup> They report a SARs incubation period of 2 to 7 days, with most infected individuals either recovering after 7 to 10 days, or dying. The SARS mortality rate is 4 percent or more. They estimate a basic reproductive number  $R_0 = 1.2$ . They model a diagnosis rate and diagnosed state. Individuals recover at a fast rate if diagnosed (8 days without diagnosis, 5 days with diagnosis).

quarantined (setting aside individuals who are exposed) and isolation (setting aside individuals who are infectious, often called hospitalization). In our model, quarantine is similarly case dependent, but can only depend on observed health status.

Empirically, the literature has begun to document the rate of transmission and incubation periods. Wu et al. (2020) compile a summary of  $R_0$  across various viruses (SARS-CoV, MERS-CoV, Commonly circulating human CoVs (229E, NL63, OC43, HKU1)), and estimate an SEIR model with international travel. Using data from the early days of the outbreak in Wuhan, they report an  $R_0$  of 2.68 and an incubation period of 6.1 days. The World Health Organization (2020) report that the time from symptom recovery to detection fell from 12 days in early January to 3 days in early February 2020. After symptom onset, it typically takes 2 weeks for a mild case to recover, or 3 to 6 weeks for severe cases.

The applied literature has also begun to document the role of quarantine in reducing transmission, and the rate of asymptomatic transmission. Kucharski et al. (2020) estimate that in China, the basic reproductive rate  $R_0$  fell from 2.35 one week before travel restrictions on Jan 23, 2020, to 1.05 one week after travel restrictions. They use an estimated SEIR model to forecast the epidemic in China, extending the model to explicitly account for infections arriving and departing via flights. Using data from Wuhan, Wang et al. (2020) report a baseline reproductive rate of 3.86, that fell to 0.32 after the vast lock-down intervention. They also find a high rate of asymptomatic transmission, leading us to consider the asymptomatic state to be infectious as opposed to the baseline SEIR model which assumes that the ‘exposed’ state is non-infectious.<sup>7</sup> A 50% rate of asymptomatic infections has been identified in Iceland, one of the few countries to adopt random testing of asymptomatic individuals.<sup>8</sup> Meta-analysis of both published and unpublished papers in Byambasuren et al. (2020) includes a wide range of asymptomatic cases, ranging from 6% to 41%.

In the recent economics literature Atkeson (2020b) and Fernández-Villaverde and Jones (2020) provide a review of the SIR model. Fenichel (2013) compares social planner and decentralized solutions for lock-down in an SIR model where all individuals recover. Alvarez et al. (2020), and Farboodi et al. (2020) study optimal lock-down policy in SIR models with the possibility of death. The latter compares the solution of the planner’s problem to a decentralized equilibrium in which individuals choose their level of engagement with the economy understanding the health risks they face. Eichenbaum et al. (2020), Jones et al. (2020) and Glover et al. (2020) nest a similar SIR model in quantitative general equilibrium macroeconomic models of consumption, savings and labor supply. The latter includes heterogeneity by age, income and assets with age-varying transmission and mortality risk. These papers consider lock-down as the only available tool to the policy-maker. Our contribution is to enrich the underlying SEIR model by introducing scope for testing policies. These policies can mitigate the output costs of broad quarantine policies while not exacerbating public health outcomes. It would be relatively straight-forward to integrate the information structure of our model into these models in order to evaluate the economic benefits of broad based testing.

Several contemporaneous papers consider testing in an SEIR model. Recent work by Piguillem and Shi (2020), Hornstein (2020), Acemoglu et al. (2020) and Brotherhood et al. (2020) study testing regimes in combination with targeted quarantine. Hornstein (2020) incorporates tracing, while Acemoglu et al. (2020) consider optimal age-dependent lockdown policies under different virological testing regimes. Similarly, Brotherhood et al. (2020) study various combinations of virological testing and age-dependent quarantine policies in a model with optimizing agents. We contribute to the literature by studying the output-death tradeoff and how it is altered by targeted quarantine, virological testing, and serological testing in a model with permanently asymptomatic individuals.

## 2. Cases, deaths, and testing through August 27, 2020

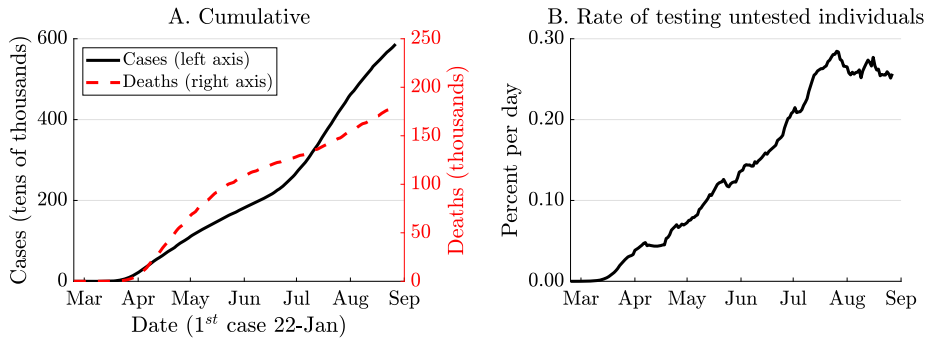
This section provides a short overview of the evolution of the COVID-19 pandemic in the United States through August 27, 2020.

The first case was reported in the U.S. on January 22, 2020. Panel A of Fig. 2 plots the evolution of confirmed COVID-19 cases up to the end of August, 2020. Despite 30 percent growth rates of cases throughout March the growth rate of cases declined up until mid-June and then began to increase again. Due to the general lack of testing in the U.S., particularly of asymptomatic individuals, confirmed cases are a noisy underestimate of the spread of COVID-19 (e.g. see Hortaçsu et al. (2020) and Stock (2020)). We will therefore focus on mortality data when calibrating and evaluating our model framework. Panel A of Fig. 2 also plots the cumulative number of deaths attributed to COVID-19 in red. Similar to case counts, the growth rate of deaths declined up until around the end of June, and then began increasing again in the second wave of the virus.

In response to the virus the US has run more than 60 million tests as of the end of August, while early on in the pandemic states issued stay-at-home orders that quarantined many individuals. Panel B of Fig. 2 reports the daily testing rate. At its peak to date, the US tested around 0.3 percent of its untested population in a single day. If testing continued at this level and were at random, each individual would be tested around once every 11 months. We consider testing levels between weekly and quarterly.

<sup>7</sup> <https://www.medrxiv.org/content/10.1101/2020.03.03.20030593v1>.

<sup>8</sup> <https://www.buzzfeed.com/albertonardelli/coronavirus-testing-iceland>. “Early results from deCode Genetics indicate that a low proportion of the general population has contracted the virus and that about half of those who tested positive are non-symptomatic”.



Notes: Source: Panel A. John Hopkins CSSE, <https://github.com/CSSEGISandData/COVID-19>. Panel B. Based on reporting by the New York Times: <https://www.nytimes.com/interactive/2020/us/coronavirus-stay-at-home-order.html>. 7 day moving average reported. In both panels, tick marks correspond to the first day of the month.

Fig. 2. Cases, deaths and testing rate.

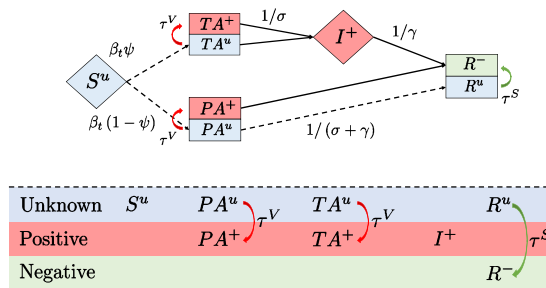


Fig. 3. SEIR model with incomplete information and testing of asymptomatic individuals.

### 3. Model

Throughout this section Fig. 1 and Fig. 3 may be useful to the reader. Fig. 1 is a non-technical schematic of our model (left), and illustrates how the model nests the standard SEIR model (right). Fig. 3 provides technical detail underlying the model, including notation and information states.

#### 3.1. Overview

There are five health states in our model (susceptible, temporary asymptomatic, permanent asymptomatic, infected symptomatic, and recovered), three information states (unknown, known positive, and known negative), and two quarantine states (quarantine, non-quarantine).

*Health states.* We base this discussion on Fig. 3, and we explain how our health states nest the standard SEIR model.

- Susceptible ( $S$ ) - These are individuals that have not been exposed to the virus. This corresponds to  $S$  in the SEIR model.
- Temporary Asymptomatic ( $TA$ ) - Individuals that have contracted COVID-19 and are temporarily asymptomatic. These individuals will eventually develop symptoms. This corresponds to  $E$  in the SEIR model: *Exposed*. Relative to the SEIR model we allow that these individuals may also transmit the virus albeit at a (potentially) lower rate.
- Permanent Asymptomatic ( $PA$ ) - Individuals that have contracted COVID-19 and will never develop symptoms. These individuals transmit the disease. There is no corresponding state in the SEIR model.
- Infected Symptomatic ( $I$ ) - Individuals that have contracted COVID-19 and are now showing symptoms. These symptoms are such that the individual knows that they have the disease and can respond to this by self-quarantining.<sup>9</sup> This corresponds to  $I$  in the SEIR model: *Infectious*. These individuals transmit the disease, potentially at a higher rate than the asymptomatic.

<sup>9</sup> This appears to attribute a certain amount of altruism to the infected. Quarantine will be imperfect which can be viewed as standing in for less than perfectly altruistic behavior. Regardless, we think such altruism is not a poor assumption. Assuming that infected people instead have nothing left to lose can lead to perverse results such as testing leading to *higher infections*. We don't think this is reasonable.

- Recovered ( $R$ ) - All individuals who previously contracted COVID-19 and have entered the recovery phase. As in the textbook SEIR model we assume these individuals are immune and do not transmit the disease.<sup>10</sup> This corresponds to  $R$  in the SEIR model: *Recovered*.

Fig. 1 (left) tracks an individual case through these states. In terms of *medical transmission*, we assume that temporary asymptomatic, permanent asymptomatic, and infected symptomatic individuals are contagious, although with potentially different rates of transmission.

Fig. 1 (right) illustrates how our model nests the SEIR model. The different rates of transmission nest the case that only infected symptomatic ( $I$ ) individuals can transmit the disease, which is the case in the SEIR model. Recovered ( $R$ ) and susceptible ( $S$ ) individuals cannot transmit the disease.

The medical block of the model is very simple and could be enriched in many ways.<sup>11</sup> We assume that susceptible individuals are infected at time varying endogenous rate  $\beta_t$ . A fraction  $\psi$  of newly infected individuals will eventually develop symptoms and are thus temporarily asymptomatic. The remaining  $1 - \psi$  of new infections never develop symptoms and are permanently asymptomatic. Asymptomatic individuals have no mortality risk. At rate  $1/\sigma$ , the temporary asymptomatic develop symptoms and transition into the infected symptomatic state from which they recover at rate  $1/\gamma$  and die at a rate  $\omega_D$ . Permanently asymptomatic cases recover at rate  $1/(\gamma + \sigma)$  so have the same expected duration of infection as those on the temporarily asymptomatic branch.

*Information.* Information is incomplete, with the environment described in Fig. 3. There are three information sets (1) unknown ( $u$ ), (2) known positive (+), and (3) known negative (−), denoted by super-scripts. Absent testing, the unknown set consists of the susceptible ( $S^u$ ), both types of asymptomatic ( $TA^u, PA^u$ ), and those that have recovered from permanently asymptomatic infection ( $R^u$ ). We are assuming that the development of symptoms is sufficient to infer a known negative recovery ( $R^-$ ). The set of known positive cases are the identified asymptomatic cases ( $TA^+, PA^+$ ), and the symptomatic state ( $I^+$ ). When assessing quarantine and testing policy, we assume that the planner cannot distinguish health-states within information sets.

*Meetings and transmission.* The underlying parameters consist of an explicit interaction of *social meeting rates*, which are mutable to quarantine/social distancing policies, and *medical transmission rates*, which determine the probability of transmission between two individuals that meet. We assume a linear matching technology, which we think is important for an assessment of serological testing, since it implies that recovered individuals mixing in the population lower infection rates.

We denote quarantine and non-quarantine states by  $Q$  and  $NQ$ , respectively. There are many feasible combinations of health states, quarantine states, and information sets. To keep the model tractable, we make the following assumptions which reduce the number of feasible states to 12:

1. **Full quarantine of known positive cases:** Known positive cases (temporary asymptomatic, permanent asymptomatic, symptomatic) are immediately quarantined. Thus there is only one state each for known temporary asymptomatic  $TA_Q^+$ , known permanent asymptomatic  $PA_Q^+$  and known symptomatic  $I_Q^+$ .
2. **Full release of known immune cases:** Since they are immune, known negative (recovered) individuals are de-quarantined immediately. Thus there is only one known recovered state  $R_{NQ}^-$ .

Susceptible individuals that test negative to a virological test are only negative that instant, so are not treated differently to untested cases. We relax the second assumption in Section 7, requiring a serological test for release (immunity passport).

The *meeting rate* of non-quarantined individuals is given by  $\lambda \in (0, 1)$ . Quarantine is imperfect, such that the meeting rate for quarantined individuals is  $\lambda^Q \in (0, \lambda)$ . We interpret the ratio factor by which quarantine reduces the rate of social interaction ( $\lambda^Q/\lambda$ ) as the time-invariant *quarantine technology* and treat it as a parameter to be calibrated.

We denote the *transmission rates* by  $\rho^A(\rho^I)$  for asymptomatic (infected symptomatic) cases to accommodate the possibility that transmission rates are higher in symptomatic cases; a key robustness exercise. These give the probability that, conditional on meeting an asymptomatic or symptomatic individual, a non-infected individual contracts COVID-19. Crucially, individuals do not know who is infected, and do not know that they have met an infected person.

*Testing.* The presence of temporary and permanent asymptomatic individuals introduces a role for both virological and serological testing. Virological tests identify active cases of the virus. Serological tests identify antibodies and thus past cases of the virus. Our information structure has assumed that when symptoms present, the individual and society know that the individual is infected. In this paper we do not cover testing of symptomatic individuals.<sup>12</sup>

<sup>10</sup> Ota (2020) tested repeated infection of SARS COV-2 in four Rhesus monkeys and found immunity to reinfection in each case. Existing human studies are inconclusive and suggest that reinfection may occur, e.g. Wen et al. (2020).

<sup>11</sup> See <http://gabgoh.github.io/COVID/index.html> by Gabriel Goh for an example of an SEIR model of *Transmission Dynamics* that appends a rich model of *Clinical Dynamics* which models hospitalization, length of hospital stay, and more.

<sup>12</sup> In our model if we were to test symptomatic individuals then all tests would yield positives. In the data a small fraction of tests yield positives. In the US our interpretation of this is not that the US is testing asymptomatic people, but rather that individuals with similar symptoms due to common colds

Virological tests allow the planner to identify and quarantine asymptomatic spreaders. We assume that virological testing of unknown cases takes place at a rate  $\tau^V$ . Known positives are immediately quarantined. In our benchmark environment, virological tests are 100 percent accurate and do not produce false negatives or false positives. For a given testing rate  $\tau^V$ , it is straight-forward to model false negatives. Since symptomatic individuals are known, a false negative is only relevant when a test is applied to an asymptomatic individual. A false negative test of an asymptomatic individual results in misclassification of the individual as unknown. This is isomorphic to simply reducing the testing rate by a pre-determined factor. In section 5 we consider false negative rates of up to 50%. False positives are rare and unlikely to pose a threat to public health policy since they simply result in overly strict quarantine, and so we preclude the occurrence of false positives.<sup>13</sup>

The only known negatives we allow for are known recovered individuals. Thus, when an individual is tested virologically and the test yields a negative result, we treat the individual as ‘unknown.’ This is to capture the notion that the test can only reveal their health state at a given point in time. Therefore, all non-infected individuals are considered unknown, regardless of whether they have just been tested or not.<sup>14</sup>

Serological tests allow the planner to identify and release known negative cases. We assume that serological testing of unknown cases takes place at a rate  $\tau^S$ . In our benchmark environment, we also assume serological tests are 100 percent accurate and do not produce false negatives or false positives.

*Quarantine.* We allow for a quarantine policy that is allowed to be targeted toward different information sets. We assume in the benchmark a *targeted quarantine* program through which known positives self-quarantine immediately and for the duration of their infection. We also assume a *targeted release* program through which known negative cases are released immediately. The only policy parameters are the rate at which unknown cases are put into quarantine ( $\xi^u$ ), and the rate at which unknown cases are released ( $\iota_t^u$ ), which we refer to as the *reopening rate*. In the next section, we take the model to the data and allow the reopening rate to be time-varying and respond to deaths in order to match the data.

### 3.2. Transmission

Given the above description of the model, we describe transition rates of individuals between states. We work in continuous time.<sup>15</sup> There is initially a unit mass of individuals. An initial mass of infected individuals  $I_0$  is distributed across  $TA^u$  and  $PA^u$  in proportions  $\psi$  and  $(1 - \psi)$ , respectively. State variables sub-scripted by  $t$  denote masses, e.g.  $S_{t,NQ}^u$  is the mass of individuals at date  $t$  who are susceptible, unknown, and non-quarantined. We denote aggregated masses of individuals in a state  $X$  in period  $t$  as  $M_t^X$ , e.g.  $M_t^Q$  is the mass of individuals in quarantine.

*Social interaction.* In order to transmit the disease, individuals must first meet. We assume random matching governed by a linear matching technology. Non-quarantined individuals meet other individuals at rate  $\lambda$ , while quarantined individuals meet others at rate  $\lambda^Q$ .

The conditional probabilities of meetings are as follows. The mass of individuals that are out in the world to bump into is given by  $M_t$ , which depends on the mass of individuals that are non-quarantined ( $M_t^{NQ}$ ) and quarantined ( $M_t^Q$ ):  $M_t = \lambda M_t^{NQ} + \lambda^Q M_t^Q$ . The masses of non-quarantined and quarantined individuals are given by,

$$\begin{aligned} M_t^{NQ} &= S_{t,NQ}^u + TA_{t,NQ}^u + PA_{t,NQ}^u + R_{t,NQ}^u + R_{t,NQ}^- \quad , \\ M_t^Q &= S_{t,Q}^u + TA_{t,Q}^u + PA_{t,Q}^u + TA_{t,Q}^+ + PA_{t,Q}^+ + R_{t,Q}^u + I_{t,Q}^+ . \end{aligned}$$

Of these, the masses of non-quarantined and quarantined individuals who can transmit the disease are

$$M_t^{I,NQ} = TA_{t,NQ}^u + PA_{t,NQ}^u \quad , \quad M_t^{I,Q} = TA_{t,Q}^u + PA_{t,Q}^u + TA_{t,Q}^+ + PA_{t,Q}^+ + I_{t,Q}^+ .$$

Conditional on meeting someone, the probability the person is infected is

$$\pi_t = \frac{\lambda M_t^{I,NQ} + \lambda^Q M_t^{I,Q}}{M_t} .$$

The conditional probabilities that the meeting is with an asymptomatic ( $\pi_t^A$ ) or symptomatic ( $\pi_t^I$ ) individual are

$$\pi_t^A = \frac{\lambda(TA_{t,NQ}^u + PA_{t,NQ}^u) + \lambda^Q(TA_{t,Q}^u + PA_{t,Q}^u + TA_{t,Q}^+ + PA_{t,Q}^+)}{\lambda M_t^{I,NQ} + \lambda^Q M_t^{I,Q}} \quad , \quad \pi_t^I = \frac{\lambda^Q I_{t,Q}^+}{\lambda M_t^{I,NQ} + \lambda^Q M_t^{I,Q}} .$$

and the flu are being tested, as well as individuals testing out of precaution. To introduce testing of symptomatic individuals one would want to extend the model to introduce an additional disease that presents observationally identical symptoms that can then be separated by testing.

<sup>13</sup> Specificity is inversely proportional to false positives (specificity=true negative/(true negative+false positive)). Sensitivity is inversely proportional to false negatives, (sensitivity = true positive/(true positive+ false negative)). In lab settings, PCR tests produce 100% sensitivity and 96% specificity, e.g. <https://spectrum.ieee.org/the-human-os/biomedical/diagnostics/testing-tests-which-covid19-tests-are-most-accurate>. Although in the field, the specificity and sensitivity are reported to be lower, e.g. <https://theconversation.com/coronavirus-tests-are-pretty-accurate-but-far-from-perfect-136671>.

<sup>14</sup> In the working paper version of this paper, we consider the opposite extreme in which testing programs reveal subsequent health transitions.

<sup>15</sup> When simulating the model we implement a discrete time approximation in which a period is one hour and days are 14 hours long.

*Infection.* A meeting with an asymptomatic (symptomatic) infected individual has a  $\rho^A$  ( $\rho^S$ ) probability of virus transmission. Once infected, an individual does not know that they are infected as they are initially asymptomatic. Independent of who they meet, if they contract COVID-19, nature exogenously determines if they will eventually develop symptoms. A newly infected individual becomes temporarily asymptomatic with probability  $\psi$  and permanently asymptomatic with probability  $1 - \psi$ . Those who are temporarily asymptomatic develop symptoms at rate  $1/\sigma$ . Once they develop symptoms they recover at rate  $1/\gamma$  or die at rate  $\omega^D$ .

*Transmission rate.* Combining the above, the rate of infection of a quarantined (non-quarantined) person is given by  $\lambda^Q \alpha_t$ , ( $\lambda \alpha_t$ ), where  $\alpha_t$  is the probability of infection conditional on a random meeting:

$$\alpha_t = \pi_t \left[ \pi_t^I \rho^I + \pi_t^A \rho^A \right].$$

We then adjust this transmission rate by the quarantine effectiveness to obtain the rate of new infection among non-quarantined  $\beta_t^{NQ}$  and quarantined  $\beta_t^Q$  individuals:

$$\beta_t^{NQ} \equiv \lambda \alpha_t \quad , \quad \beta_t^Q \equiv \lambda^Q \alpha_t.$$

### 3.3. Transition rates

We describe the full set of transition rates between all 13 states in Table 1. Along with initial conditions for the distribution of individuals across health and information states, these transition rates are sufficient to simulate the model. We provide examples of three states:  $S_{NQ}^u$ ,  $TA_{NQ}^u$  and  $R_Q^u$ .

*Susceptible, unknown.* All non-infected individuals are unknown, regardless of whether they have been tested. Three events can affect an unknown susceptible individual. At rate  $\beta_t^{NQ}$  the individual is infected with COVID-19; a product of their meeting rate  $\lambda^{NQ}$ , the probability of a meeting  $\pi_t$ , and the conditional probability of infection  $\pi_t^I \rho^I + \pi_t^A \rho^A$ . Conditional on infection the individual becomes  $TA^u$  with probability  $\psi$ , and  $PA^u$  with probability  $(1 - \psi)$ . At rate  $\xi^u$  the individual is put into quarantine and transitions to  $S_{NQ}^u$ . Note that at rate  $\tau^V$  ( $\tau^S$ ) the individual receives a virological test which reveal that the individual is not (has not been) infected, and so they remain in  $S_{NQ}^u$ .

*Temporary asymptomatic, unknown.* Like the susceptible type the individual goes into quarantine at rate  $\xi^u$ . Now following a virological test, which occurs at rate  $\tau^V$ , the individual tests positive and is quarantined  $TA_Q^+$ . From  $TA_Q^+$  they transition to the infected state, still under quarantine, and then become a known recovery and so are released. At rate  $1/\sigma$ , the individual develops symptoms before being tested, and transitions to  $I_Q^+$ .

*Recovered unknown, quarantine.* Due to porous quarantine, early cases and the permanently asymptomatic route, some individuals will contract Covid-19 without knowing it and be recovered while still being quarantined. While a virological test at rate  $\tau^V$  reveals nothing, at rate  $\tau^S$  these individuals receive a serological test which reveals antibodies. At this point the individual moves into the absorbing state  $R^-$  which is in the known negative information set and so is released from quarantine.

*Nesting the SEIR and SIR models.* Formally, the SEIR model is nested under the following parameter restrictions: (i) no quarantine ( $\lambda/\lambda^Q = 1$ ,  $\xi^u = 0$ ,  $r_t^u = \infty$ ), (ii) no asymptomatic transmission ( $\rho_A = 0$ ), (iii) no permanent asymptomatic infection ( $\psi = 1$ ), (iv) no testing ( $\tau^V = \tau^S = 0$ ). In this case, individuals move from  $S_{NQ}^u \rightarrow TA_{NQ}^u \rightarrow I_Q^+ \rightarrow R_{NQ}^-$ , which substantively correspond to the SEIR states.

### 3.4. Vaccine and anti-viral

We assume an arrival of a vaccine/anti-viral at a fixed future date. We assume the vaccine/anti-viral is distributed at rate  $\nu$ . In the exercises that follow, we model vaccine such that  $\nu_t = 0$  up until some date  $\tau$ , then  $\nu_t = \nu$  for  $t > \tau$ . For the susceptible, treatment delivers a transition to known recovered and non-quarantined. For known and unknown, temporary and permanent asymptomatic cases, treatment delivers a transition to known permanent asymptomatic.

### 3.5. Measurement

#### 3.5.1. Basic reproduction number

We consider two measures of the basic reproduction numbers summarized by Cori et al. (2013). One is based on a hypothetical date 0 case, *ceteris paribus*, in particular, holding policy and contact rates fixed: *Cori method*. The other is based on the realized path of infections generated along the transition path: *Wallinga–Teunis method* (Wallinga and Teunis, 2004). The difference parallels a comparison of *predicted* (Cori) and *realized* (Wallinga–Teunis) life expectancy in demographics for any given cohort.

**Table 1**  
Poisson transition rates.

A. Initial	B. Next instant state												
	Susceptible		Temporary asymp.			Infected symp.	Permanent asymp.			Recovered			Dead
	$S_{NQ}^u$	$S_Q^u$	$TA_{NQ}^u$	$TA_Q^u$	$TA_Q^+$	$I_Q^+$	$PA_{NQ}^u$	$PA_Q^u$	$PA_Q^+$	$R_{NQ}^u$	$R_Q^u$	$R_{NQ}^-$	$D$
$S_{NQ}^u$		$[\xi^u]$	$\beta_t^{NQ} \psi$				$\beta_t^{NQ} (1 - \psi)$						$v_t$
$S_Q^u$	$(r_t^u)$			$\beta_t^Q \psi$				$\beta_t^Q (1 - \psi)$					$v_t$
$TA_{NQ}^u$				$[\xi^u]$	$\tau^V$	$1/\sigma$				$v_t$			
$TA_Q^u$			$(r_t^u)$		$\tau^V$	$1/\sigma$				$v_t$			
$TA_Q^+$						$1/\sigma$							
$I_Q^+$												$1/\gamma$	$\omega^D$
$PA_{NQ}^u$										$\tau^V + v_t$	$\frac{1}{\sigma + \gamma}$		
$PA_Q^u$							$(r_t^u)$	$[\xi^u]$		$\tau^V + v_t$	$\frac{1}{\sigma + \gamma}$		
$PA_Q^+$												$\frac{1}{\sigma + \gamma}$	
$R_{NQ}^u$											$[\xi^u]$		$\tau^S + v_t$
$R_Q^u$										$(r_t^u)$			$\tau^S + v_t$
$R_{NQ}^-$													

Notes: In any instant only one transition can occur. The red  $[\xi^u]$  terms are rates into quarantine. The green  $(r_t^u)$  terms are rates out of quarantine, which represent reopening policy and are varied in our counterfactuals.

*Cori method.* Consider a hypothetical ‘date-zero’ case of an individual that has just contracted COVID-19, and nature is yet to determine if they are temporarily or permanently asymptomatic. A summary statistic of the disease is the expected number of infections caused by this single infected person:  $R_0^C$ . We can write  $R_0^C$  recursively as follows.

Consider an initial temporary asymptomatic case, before any quarantine measures go into effect. At rate  $\lambda$  they meet another individual and with probability  $\rho^A$  they transmit the disease. At rate  $\sigma^{-1}$  the individual develops symptoms. Once the individual has developed symptoms, they meet others at rate  $\lambda$  and transmit the disease with probability  $\rho^S$ . The resulting recursive equations for the number of infections generated by this date-zero case are:

$$R_0^{A,Temp,NQ} = \lambda \rho^A + (1 - \sigma^{-1}) R_0^{A,Temp,NQ} + \sigma^{-1} R_0^{I,NQ},$$

$$R_0^{I,NQ} = \lambda \rho^S + (1 - \gamma^{-1} - \omega^D) R_0^{I,NQ}.$$

We can solve this system of equations for the expected number of cases generated by the initial temporarily asymptomatic case:

$$R_0^{A,Temp,NQ} = \left[ \sigma \lambda \rho^S \left[ \frac{\rho^A}{\rho^S} + \frac{\sigma^{-1}}{\gamma^{-1} + \omega^D} \right] \right] \tag{1}$$

Now consider an initial permanent asymptomatic individual. At rate  $\lambda \rho^A$ , the individual meets someone and transmits the disease. At rate  $(1 - (\sigma + \gamma)^{-1})$ , they do not recover. We can express the number of infections generated by this date zero case recursively and solved for:

$$R_0^{A,Perm,NQ} = \lambda \rho^A + (1 - (\sigma + \gamma)^{-1}) R_0^{A,Perm,NQ} = (\sigma + \gamma) \lambda \rho^A \tag{2}$$

Since nature ultimately determines if the initial infection is temporarily or permanently asymptomatic, the overall Cori-method basic reproductive number  $R_0^C$  is given by:

$$R_0^C = \psi R_0^{A,Temp,NQ} + (1 - \psi) R_0^{A,Perm,NQ}$$

Combining (1) and (2) delivers the number of infections generated by a date-zero case of COVID-19:

$$R_0^C = \lambda \rho^S \left\{ \psi \left[ \sigma \left( \frac{\rho^A}{\rho^S} + \frac{\sigma^{-1}}{\gamma^{-1} + \omega^D} \right) \right] + (1 - \psi) \left[ (\sigma + \gamma) \frac{\rho^A}{\rho^S} \right] \right\} \tag{3}$$

*Wallinga-Teunis method.* By contrast, the Wallinga-Teunis method is forward-looking and takes into account the full dynamics of disease transmission. Since quarantine measures in the US started in mid-March, around the same time that case and death measurements began, this is the appropriate measure for comparing to data on Covid case transmission. Since we will ultimately solve the model using a discrete time approximation, we express the Wallinga-Teunis method using discrete time. Denote the discrete-time approximation of the transition matrix (Table 1) across the 13 health and information states

$\mathbf{P}_t$ .<sup>16</sup> Let  $\rho_t$  be a  $13 \times 1$  vector of the expected contemporaneous date  $t$  infections due to an individual in each state, and let  $\mathbf{R}_t$  be the vector of the cumulative number of these infections. After some date  $T$ , once the vaccine has completely rolled out, a new infection would generate zero cases:  $\mathbf{R}_T^{WT} = \rho_T = \mathbf{0}$ . Working backwards

$$\mathbf{R}_t^{WT} = \rho_t + \mathbf{P}_t \mathbf{R}_{t+1}^{WT} \quad , \quad t \in \{1, \dots, T-1\}. \tag{4}$$

Using the same ordering of states as in Table 1, the expected number of infections due to individuals in each state is<sup>17</sup>

$$\rho_t = \left[ 0, 0, \underbrace{\rho^A \lambda}_{\langle TA_{NQ}^u \rangle}, \underbrace{\rho^A \lambda^Q}_{\langle TA_Q^u \rangle}, \underbrace{\rho^A \lambda^Q}_{TA_Q^+}, \underbrace{\rho^S \lambda^Q}_{I_Q^+}, \underbrace{\rho^A \lambda}_{\langle PA_{NQ}^u \rangle}, \underbrace{\rho^A \lambda^Q}_{\langle PA_Q^u \rangle}, \underbrace{\rho^A \lambda^Q}_{PA_Q^+}, 0, 0, 0, 0 \right]' \times \left( \frac{\lambda S_{t,NQ}^u + \lambda^Q S_{t,Q}^u}{M_t} \right) \tag{5}$$

where the final term is the conditional probability that a meeting is with a susceptible individual.

We then obtain the desired measure, which is the expected value for a susceptible individual infected at date  $t$ . An infected individual enters one of the four states in angle brackets (5). To obtain the scalar Wallinga-Teunis measure we weight  $\mathbf{R}_t^{WT}$  by the probabilities attached to initial infection states:

$$\mathbf{R}_t^{WT} = \underbrace{\left[ 0, 0, (1 - f_t) \psi, f_t \psi, 0, 0, (1 - f_t) (1 - \psi), f_t (1 - \psi), 0, 0, 0, 0, 0 \right]}_{\pi_t} \times \mathbf{R}_t^{WT} \quad , \quad f_t = \frac{\lambda^Q S_{t,Q}^u}{\lambda S_{t,NQ}^u + \lambda^Q S_{t,Q}^u} \quad ,$$

where  $f_t$  is the conditional probability the individual was in quarantine. The key conceptual difference between the Cori and Wallinga-Teunis methods is that the former does not take into account future changes in policy and disease evolution. In the notation we set out for the Wallinga-Teunis method, the Cori method  $R_t^C$  assumes that  $\mathbf{P}_t$  is permanent:

$$\mathbf{R}_t^C = \rho_t + \mathbf{P}_t \mathbf{R}_t^C \quad , \quad \mathbf{R}_t^C = (\mathbf{I} - \mathbf{P}_t)^{-1} \rho_t \quad , \quad R_t^C = \pi_t \times \mathbf{R}_t^C$$

For example,  $R_0^{WT} < R_0^C$  if quarantining of types in the future and building of herd immunity reduces future infections.

### 3.5.2. Activity

When comparing policies, we focus on three metrics: Output, symptomatic infection, and mortality. A reasonable approximation of economic activity is that it scales with the number of non-quarantined workers. We assume that quarantined workers are  $A_{rel} \in [0, 1)$  less productive than non-quarantined workers, and symptomatic workers are incapacitated so do not produce. Output  $Y_t$  is therefore

$$Y_t = S_{t,NQ}^u + TA_{t,NQ}^u + PA_{t,NQ}^u + R_{t,NQ}^u + R_{NQ}^- + A_{rel} \left( S_{t,Q}^u + TA_{t,Q}^u + PA_{t,Q}^u + TA_{t,Q}^+ + PA_{t,Q}^+ + R_{t,Q}^u \right).$$

In the initial period all individuals are non-quarantined and the initial infected are asymptomatic, so  $Y_0 = 1$ . Therefore  $Y_t$  is in units of the percent deviation of output from the initial period. A reasonable approximation of the load on the hospital system is that it scales with the number of infected, symptomatic individuals. We therefore report symptomatic infections,  $I_t$ . The number of deaths at any instant of time is given by  $\omega^D I_t$ . We focus on the cumulative death rate.

## 4. Quantification

### 4.1. Timeline

We are interested in how testing can affect reopening and, through this, economic output. We think of the virus and response to the virus in three phases. In the *lockdown phase*, from March 20 to May 31, 2020, an exogenous quarantine policy leads to quarantining of unknown individuals at rate  $\xi^u$ . In the *reopening phase*, from June 1, 2020 to March 20, 2021, we assume that having some experience of the virus, individual behavior causes reopening to respond to the death-rate. In our counterfactuals, widespread testing is available in the reopening phase. In the *vaccine phase*, starting March 21, 2021, the vaccine is available, one year after the start of lockdowns.

This structure has two key implications. First, our counterfactuals do not assume the possibility of widespread testing from the start of the pandemic. Second, our counterfactuals incorporate an interaction between testing and reopening through individual behavior.

<sup>16</sup> With death being an absorbing state, Table 1 yields a  $13 \times 13$  transition matrix.

<sup>17</sup> In practical terms this can only be computed backward after solving the model forwards.

**Table 2**  
Model parameters and values.

Parameter		Source/Target	Value
<b>A. Medical</b>			
Daily rate at which infected become symptomatic	$1/\sigma$	6 days incubation period	1/6
Daily rate at which symptomatic recover	$1/\gamma$	8 day symptomatic period (14 day recovery)	1/8
Fraction that develop symptoms	$\psi$	Literature	0.60
Relative probability of asymptomatic transmission	$\rho^A/\rho^S$	Kimball et al (2020)	1
<b>B. Externally calibrated</b>			
Daily rate of meeting	$\lambda$	Normalized contact rate	1
Initial asymptomatic infections	$I_0$	0.1 percent of population on March 16, 2020	340,000
Relative output of quarantined	$A_{rel}$	Decline in output of 10 percent	0.90
<b>C. Internally calibrated</b>			
Daily mortality rate	$\omega^D$	Infection fatality rate of 1 percent	0.0021
Daily quarantine rate	$\xi^u$	49.5 percent pop. in quarantine on April 7, 2020	0.0364
Basic reproduction number	$R_0^C$	Cumulative deaths on April 30, 2020	2.60
Effectiveness of quarantine technology	$\lambda^Q/\lambda$	Cumulative deaths on June 15, 2020	0.16
Reopening sensitivity	$\theta$	Cumulative deaths on August 27, 2020	0.00275
Probability of transmission	$\rho^S$	Given other parameters, implies $R_0^C = 2.6$	0.013

Notes: We compound parameters in the underlying model into daily rates, which are then expressed in the table.

### 4.2. Reopening

During the reopening phase we assume that reopening responds to the death rate. Since we do not have a model of economic behavior, we achieve this through a reduced form. Below we discuss how this captures the theoretical predictions for the time-series of  $R_t$  due to Farboodi et al. (2020), which have been supported by the data (Atkeson et al., 2020). Before June 1, 2020, we assume that individuals do not exit quarantine except through recovery from a symptomatic infection. Therefore, we assume  $r_t^u = 0$  before June 1, 2020. After June 1, 2020, we model reopening as a positive flow out of quarantine. This can be viewed as a proxy for relaxation of shelter-in-place or social distancing measures. During the reopening phase, we assume that individuals exit quarantine in a way that depends on both government policy and the daily death rate. After June 1, 2020, we assume the reopening rate is given by  $r_t^u = r_t^{u,Pol} + r_t^{u,Endog}$ . The parameter  $r_t^{u,Pol}$  is a proxy for government controlled relaxation of quarantine (reopening parks, gyms, etc.), whereas  $r_t^{u,Endog}$  captures the endogenous choice to exit quarantine among individuals. We assume that this endogenous component responds to the percent deviation in deaths from June 1, 2020. The way deaths affect the rate at which individuals exit quarantine is governed by the parameter  $\theta$ :

$$r_t^{u,Endog} = \theta \max \left\{ \underbrace{\frac{\text{Daily deaths}_{\text{June 1, 2020}} - \text{Daily deaths}_{t-1}}{\text{Daily deaths}_{\text{June 1, 2020}}}}_{\text{Percent decline in deaths relative to June 1, 2020}}, 0 \right\}$$

In summary, the reopening rate  $r_t^u$  is given by the following piece-wise function:

$$r_t^u = \begin{cases} 0 & t \leq \text{June 1, 2020} \\ r_t^{u,Pol} + \theta \max \left\{ \frac{\text{Daily deaths}_{\text{June 1, 2020}} - \text{Daily deaths}_{t-1}}{\text{Daily deaths}_{\text{June 1, 2020}}}, 0 \right\} & t > \text{June 1, 2020.} \end{cases} \quad (6)$$

The parameter  $r_t^{u,Pol}$  is a policy for reopening used later in our counterfactuals, but for now consider this being set to zero. Equation (6) implies that if daily deaths exceed their daily level on June 1, 2020, the reopening rate returns to zero. When deaths are lower, reopening occurs at a rate which is increasing in the deviation of deaths from their June 1, 2020 level, with sensitivity  $\theta$ .

Why this specification? A high value of  $\theta$  will lead to a sharp rebound in deaths during the second wave of the disease which starts in mid-June (Fig. 2D). A low value will lead to a small second wave. We can therefore choose  $\theta$  to match the properties of this resurgence of the virus. If instead of (6) we simply set  $r_t^u = \theta$  and chose  $\theta$  to match the same data, then the second wave would be substantially larger than the first wave. Under (6), the reopening leads deaths to increase, which reduces reopening, leading to a flattening of the second wave. This will not be directly targeted, but turns out to be consistent with the data. We therefore think of this functional form as being informed by the data.

### 4.3. Parameters

Parameter values are given in Table 2. The parameters of the model can be classified into two groups. The first relates to *medical* parameters, which would be the equivalent of technological parameters in an economic model. We use existing

medical studies to inform these parameters. Since a number of recent papers have discussed significant measurement challenges for medical parameters, e.g. Atkeson (2020a), Stock (2020) and Hortaçsu et al. (2020), we consider robustness of our conclusions to these parameters in Section 7. The second set of parameters is jointly calibrated to match features of the data. Throughout this section, we convert to daily rates.<sup>18</sup> The benchmark features no testing.

*Initial conditions.* We seed initial infections in the U.S. on March 16, 2020 and assume that quarantine policy begins on March 20, 2020 (see Fig. B1 in Online Appendix Section B). The quarantine policy is not removed until a vaccine is introduced on March 20, 2021, which is distributed to unvaccinated individuals at a rate of 1.5 percent per day ( $\nu = 0.015$ ). There is no virological or serological testing ( $\tau^V = \tau^S = 0$ ) and no additional reopening ( $r^{u,Pol} = 0$ ). The number of initial infections  $I_0$  on March 16, 2020 is set to 0.1 percent of the U.S. population:  $I_0 = 340,000$ . Official data reports 4,354 cases on March 16, so we are assuming this represents 1.5 percent of all cases. This is the rate of under-reporting derived by Hortaçsu et al. (2020) for March 9, 2020 (Table 3, Panel 2).

*Medical parameters.* The daily rate at which infected individuals transition from asymptomatic to symptomatic cases,  $1/\sigma$ , is such that the average incubation period is 6 days (Wu et al., 2020). World Health Organization (2020) report that the average recovery period is 14 days for mild infections. We therefore set  $\gamma$  so that symptoms last for 8 days so that expected time from infection to recovery is 14 days. We shorten and lengthen these durations in Online Appendix Section A.

The fraction of individuals who never develop symptoms is given by evidence that roughly 40 percent of individuals are permanently asymptomatic:  $\psi = 0.6$ .<sup>19</sup> Recent evidence on the relative transmissibility of asymptomatic and symptomatic cases is provided by Kimball et al. (2020). They study disease transmission in a skilled nursing home and are unable to statistically distinguish differences in viral loads between asymptomatic and symptomatic individuals. Therefore in our benchmark asymptomatic and symptomatic individuals transmit the disease at the same rate:  $\rho^A/\rho^S = 1$ .<sup>20</sup>

*Calibrated.* We are left with the following parameters to calibrate:  $\{\lambda, \rho^S, A_{rel}, \omega^D, \lambda^Q, \xi^u, \theta\}$ . As shown by equation (3),  $\lambda$  and  $\rho^S$  are not separately identified. We therefore set  $\lambda = 1$  and back out the implied  $\rho^S$  that is consistent with a value of  $R_0^C$  using the Cori-method. We treat  $R_0^C$  as an auxiliary parameter to be estimated. We set  $A_{rel} = 0.90$  such that the benchmark decline in US GDP is 10 percent, which replicates the year-on-year decline in second quarter real GDP from the BEA.<sup>21</sup>

We jointly calibrate the (i) the mortality rate  $\omega^D$ , (ii) quarantine rate  $\xi^u$ , (iii) quarantine technology  $\lambda^Q$ , (iv) reproduction number  $R_0^C$ , and (v) reopening sensitivity  $\theta$  in order to target (1) the infection fatality rate, (2) the population under quarantine on April 7, 2020, and (3,4,5) the number of deaths on April 30, June 15, and August 27, 2020. Given values for  $\psi, \rho^A/\rho^S, \sigma, \gamma, \omega^D$ , and the normalization of  $\lambda$ , we use equation (3) to solve for the  $\rho^S$  that yields the conjectured value of  $R_0^C$ .<sup>22</sup>

*Estimates.* We target an infection fatality rate of 1 percent, which is in line with the infection fatality rate in New York computed as deaths divided by total infections, where total infections are measured using serological test results.<sup>23,24</sup> We obtain an estimated mortality rate  $\omega^D = 0.0021$ . In our robustness exercises we show our results are unchanged by changing this moment to 0.5 or 1.5 percent.

As discussed in Online Appendix Section B, the fraction of the U.S. population living in states with some form of stay-at-home order peaked at 90 percent on April 7, 2020. Of course, not all individuals in those states actually entered quarantine. Many essential sector workers continued to work, as well as non-compliers. Following Glover et al. (2020), who refer to this as the ‘basic sector’, we assume that 45 percent of workers are in the basic sector and that workers in the basic sector do not enter quarantine. Our estimate  $\xi^u = 0.0364$  per day matches 49.5 percent ( $= 0.90 \times (1 - 0.45)$ ) of the population in quarantine as of April 7, 2020.

<sup>18</sup> The discrete time approximation used to solve the model is with one period equal to one hour, and 14 hours per day.

<sup>19</sup> This is the *upper bound* of estimates in the survey by Byambasuren et al. (2020). We report robustness with respect to the fraction that are permanently asymptomatic in Section 7, considering  $\psi \in \{0.50, 0.75\}$ .

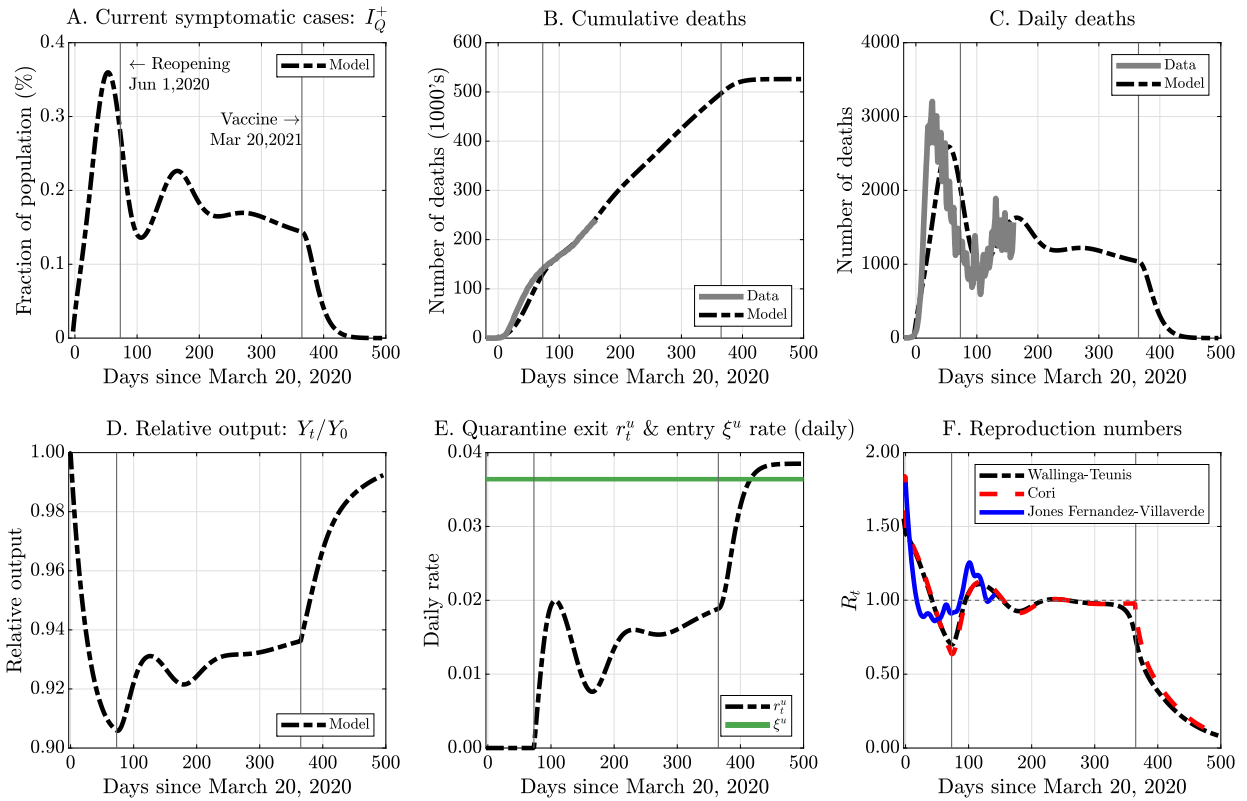
<sup>20</sup> Furukawa et al. (2020) provides a review of pre-symptomatic and asymptomatic viral loads (cycle thresholds). These cycle thresholds determine infectiousness. The cycle threshold is inversely proportional to the viral load. After conducting viral load tests in a long-term care skilled nursing home, Kimball et al. (2020) describe an inability to distinguish differences in viral loads between asymptomatic and symptomatic individuals, although their samples sizes and power of tests are low. Kimball et al. (2020) write, “The reverse transcription–polymerase chain reaction (RT-PCR) testing cycle threshold (Ct) values indicated large quantities of viral RNA in asymptomatic, presymptomatic, and symptomatic residents, suggesting the potential for transmission regardless of symptoms... Real-time RT-PCR Ct values for both genetic markers among residents with positive test results for SARS-CoV-2 ranged from 18.6 to 29.2 (symptomatic [typical symptoms]), 24.3 to 26.3 (symptomatic [atypical symptoms only]), 15.3 to 37.9 (presymptomatic), and 21.9 to 31.0 (asymptomatic). There were no significant differences between the mean Ct values in the four symptom status groups ( $p = 0.3$ ).”

<sup>21</sup> See: <https://fred.stlouisfed.org/graph/?g=tEQJ>.

<sup>22</sup> We can match the first two moments exactly. We minimize the total absolute percent deviations of the data and model across the death moments.

<sup>23</sup> We refer readers to Fernández-Villaverde and Jones (2020) for a thorough discussion of infection fatality rate estimates.

<sup>24</sup> It is important to note that  $\omega^D$  does not correspond to the *case fatality rate*, where the case fatality rate is defined to be the ratio of cumulative deaths to cumulative cases. “In epidemiology, a *case fatality rate* (CFR) – sometimes called *case fatality risk* or *case-fatality ratio* – is the proportion of deaths from a certain disease compared to the total number of people diagnosed with the disease for a certain period of time.” (Wikipedia).



Notes: Vertical lines separate out time into the three phases discussed in the text: (i) lockdown, (ii) reopening, (iii) vaccine.

Fig. 4. Benchmark model fit and forecast under no testing.

The dates we chose to match deaths on are designed to capture the high initial rate of growth of deaths, the flattening off of the curve and the increase in deaths as reopening began. The inflection point where cumulative deaths change from concave to convex is June 15; the mid-point of this and the start of quarantine is April 15; and the last day for which we have data is August 27. A higher  $R_0^C$  leads to a steeper path for initial deaths, a lower  $\lambda_Q$  leads to a quicker flattening off, and a higher  $\theta$  leads to a steeper increase in deaths in summer. We estimate  $R_0^C = 2.6$  and  $\lambda^Q = 0.16$ , such that quarantine reduces meetings by a factor of more than six. Our estimated value of  $R_0^C$  is in line with estimates of the basic reproductive number at the onset of the Italian and Chinese Covid-19 outbreaks (Li, Guan, Wu, et al., 2020; and Gatto, Bertuzzo, Mari, et al., 2020) and estimates from an alternative model by Fernández-Villaverde and Jones (2020) for the US. In our robustness exercises we consider alternative values of  $R_0^C \in \{2, 3\}$ . The estimated sensitivity  $\theta$  is 0.00275. When matching deaths, we follow Fernández-Villaverde and Jones (2020) and inflate mortality data by 33 percent.<sup>25</sup>

We note that our parameters are consistent with those in the current ‘Best estimates’ provided by the CDC in September 2020. These are provided by the CDC to modelers and for forecasting various different scenarios.<sup>26</sup>

#### 4.4. Model fit

In Fig. 4, we plot the path of symptomatic infected individuals, deaths, output, reproduction numbers, reopening/quarantine rates, and reproduction numbers. The vertical lines mark when reopening occurs and when the vaccine is introduced.

The model matches deaths on June 15 and August 27 exactly, but understates deaths on April 30.<sup>27</sup> The model comes close to generating the path for deaths in the data in the lockdown phase, however it is unable to generate the steep convex time-series of cumulative deaths given initial infections. Our reduced form for reopening matches the data well. By June 15, quarantine has led the reproduction number to be less than one. Consequently infections and deaths are falling. As they fall, equation (6) implies individuals move out of quarantine, and reopening is positive (Panel E). With more frequent meetings, the reproduction number increases, the disease spreads faster and infections and deaths increase. As deaths increase the

<sup>25</sup> This inflation factor captures under-reporting of deaths, and is based on excess death measures in other countries and New York City.

<sup>26</sup> See: <https://www.cdc.gov/coronavirus/2019-ncov/hcp/planning-scenarios.html>. These include:  $R_0 = 2.5$ ,  $IFR = 0.65$  percent,  $\psi = 0.60$ ,  $\rho^A/\rho^S = 0.75$ ,  $\sigma = 1/6$ , total length of infection of 15 days. We consider the case of  $\rho^A/\rho^S = 0.5$  in Section 7.

<sup>27</sup> A higher value of  $R_0^C$  could match this, but would require a lower  $\lambda^Q$  to match deaths on June 15.

economy retreats once more. The choice of  $\theta$  matches the increase in deaths in the second wave exactly, but leads the second wave to be smaller than the first. This matches the flattening off of daily deaths over August.

The reduced form model implies a time-varying path for the reproduction number that is consistent with data and theory (Panel F). The Wallinga-Teunis measure  $R_t^{WT}$  incorporates the future path of quarantine policy and thus lower infection rates, and moves ahead of the Cori measure  $R_t^C$ . In accounting for this it is markedly lower at the onset of our simulation than 2.60.<sup>28</sup> Nonetheless, both time varying paths of  $R_t^{WT}$  and  $R_t^C$  are in line with estimates for the U.S. (Atkeson et al., 2020). For comparison we plot the estimate for the US from Fernández-Villaverde and Jones (2020). Had we assumed a constant reopening rate, or a constant quarantine rate without reopening, the reproduction number would continue to increase or decrease, respectively. Both would be counterfactual. Finally, the time-series for the basic reproduction number is consistent with the theoretical predictions of Farboodi et al. (2020). In their quite general model, individuals equate marginal utility of activity that spreads the virus to the marginal health of these activities, leading to reproduction rates that hover around one.

## 5. Testing

We now introduce virological ( $\tau^V$ ) and serological testing ( $\tau^S$ ). First, we compute output and deaths under the benchmark model with testing  $\{r^{u,Pol} = 0, \tau^V > 0, \tau^S > 0\}$ . Second, we measure how much we can additionally reopen by increasing the release rate of unknown cases  $\{r^{u,Pol} > 0\}$  such that long-run level of cumulative deaths is capped at by the benchmark quarantine-only policy (Fig. 4A). Throughout we keep the endogenous component of reopening in equation (6).

We consider different rates of testing. To make sense of the testing numbers, we report the average number of weeks between tests for an unknown individual that does not become infected. For example, an average number of weeks between tests of 1 week corresponds to roughly 340 million tests per week. We change  $\tau^S$  and  $\tau^V$  such that this ranges between weekly to quarterly. We discuss feasibility of these levels in Section 8.

### 5.1. Testing without additional reopening: $r^{u,Pol} = 0$

We first illustrate the impact of virological and serological tests on output losses and deaths under our benchmark model with fixed quarantine policy  $\xi^u = 0.0364$  and no additional reopening  $r^{u,Pol} = 0$ . We consider virological and serological tests separately. Recall that if an individual has a positive virological test, we assume they enter quarantine, and if a serological test identifies antibodies we assume they are released (see Table 1).

*High frequency testing.* Fig. 5 plots medical and economic time-series for the (i) benchmark (no-testing), (ii) virological testing, and (iii) serological testing. For these figures we assume testing every two weeks. The black line in Fig. 5 traces the paths of these variables for our benchmark quarantine-only economy  $\{r^{u,Pol} = \tau^V = \tau^S = 0\}$ . Under the benchmark policy, approximately 0.35 percent of the population are symptomatic at the first peak of the pandemic (Panel A). Daily deaths peak at 2,500 per day during the first wave (Panel C). Following reopening on June 1, 2020, a second wave of the disease begins. The peak symptomatic infection rate during the second wave is approximately 0.2 percent. Daily deaths peak at 1,500 per day during the second wave.

Following the quick peaks of the first and second wave, panel D shows that the basic reproduction number hovers around 1 for a year, generating about 1,000 deaths per day until the vaccine is introduced. As a result our model predicts approximately 0.15 percent of the U.S. population dies from the disease, which is just over half a million deaths: 510,000 (Panel B).

The mid-dashed red line in Fig. 5 traces out the path of the economy when individuals are virologically tested every two weeks through the reopening phase  $\{\tau^V = 0.072, r^{u,Pol} = \tau^S = 0\}$ . The benchmark quarantine policy remains in place and additionally those with positive virological tests are quarantined. By quickly quarantining both types of asymptomatic cases, infection rates and deaths continue to fall. This leads to greater reopening which keeps  $R_t$  close to one. Despite the increase in reopening, testing keeps up with the additional spread of the disease, further lowering infections and deaths. By the time the vaccine arrives the virus is by no means dead, many more remain susceptible than the level required for herd immunity given  $R_0 = 2.60$ , but testing has kept transmission under control.

The economic and health benefits of virological testing are significant. The economic consequences of virological testing are driven by the reopening that it accommodates. As the economy reopens labor is used in production more effectively and output increases. The rebound of output is capped by the reopening response: a sharper increase in reopening would increase output, but cause deaths to increase and reopening to retreat. The health consequences of virological testing are observed in the level of deaths. Overall, the cumulative death rate falls by a factor of 3 relative to the benchmark economy.

The dotted blue line in Fig. 5 traces out the path of the economy when individuals are serologically tested every two weeks through the reopening phase  $\{\tau^S = 0.072, r^{u,Pol} = \tau^V = 0\}$ . The benchmark quarantine policy remains in place, however, those who test positive for antibodies are released. Serological testing has a muted effect on public health outcomes

<sup>28</sup> The initial Cori method reproduction number is also less than 2.60. This is explained by the fact that the  $R_0^C$  used as an auxiliary parameter in the estimation is based on there being an infinitesimal population of infected individuals, whereas in the model this is not the case.

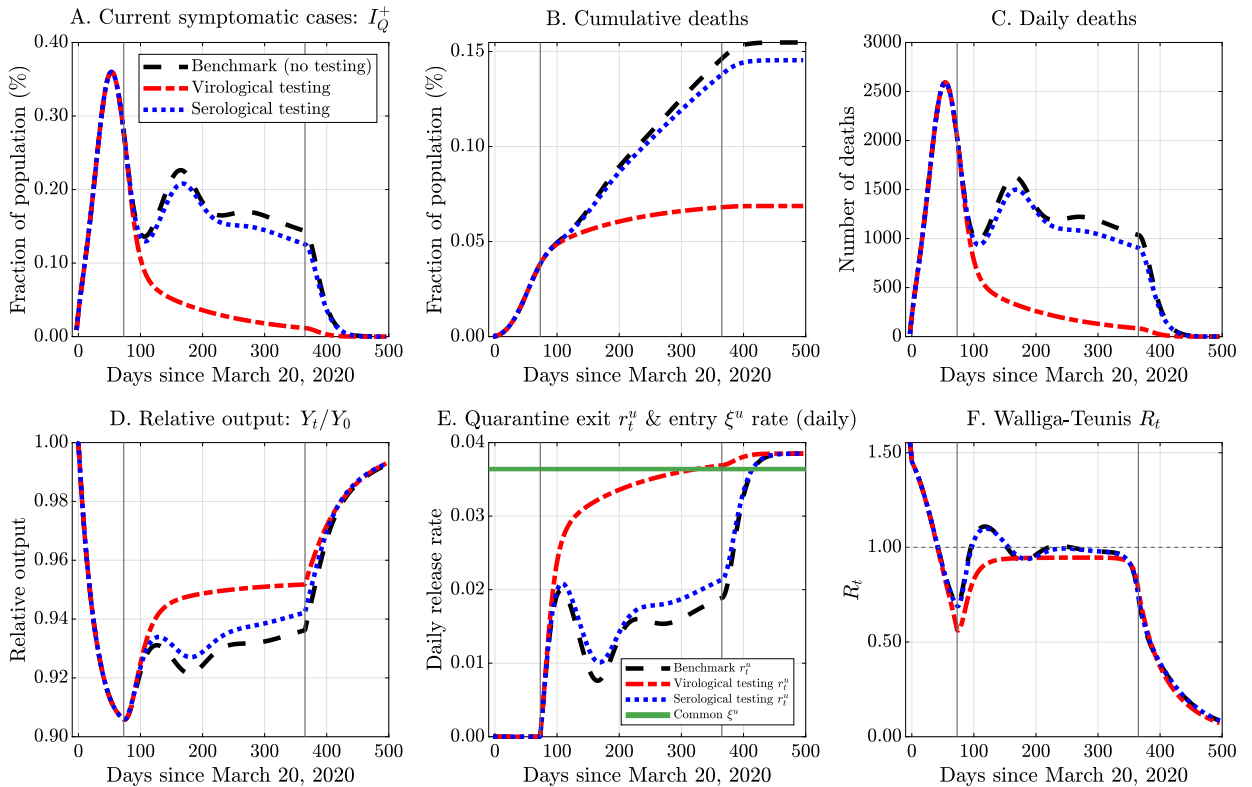


Fig. 5. Testing every two weeks without additional reopening: ( $r^{u,Pol} = 0$ ).

with a small decline in infections and deaths. This might come as a surprise: by identifying and releasing more individuals with antibodies, a greater fraction of meetings are with immune individuals which reduces disease transmission, especially given a linear matching technology. These effects are quantitatively small for the simple reason that the number of recovered individuals is small. With a small effect on deaths, reopening is also muted, and the increase in output due to the combination of reopening and the release of recovered cases is small.

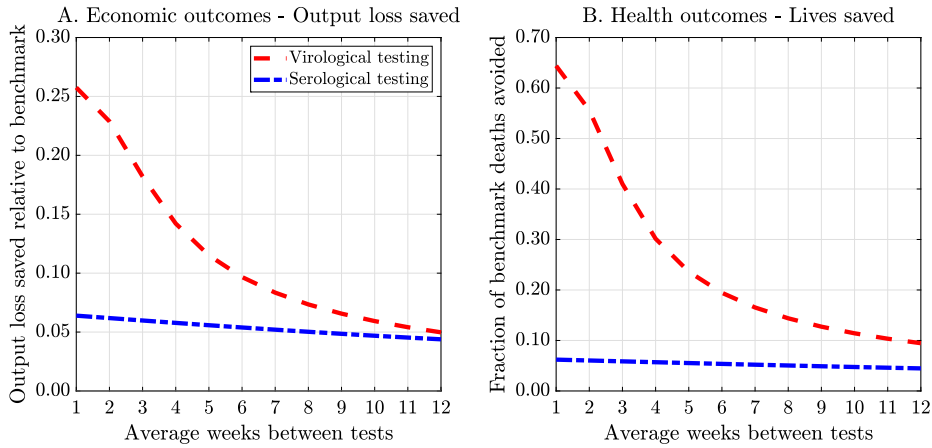
*Varying testing frequency.* We quantify how the health and economic outcomes of testing depend on the frequency of testing. Fig. 6 compares output losses and deaths as the frequency of testing varies. The x-axis reports average weeks between testing. Panel A plots the cumulative difference in output losses over reopening, before the vaccine: June 1, 2020 to March 20, 2021. We plot the output loss relative to the benchmark economy without testing, which correspond to the sum of the differences between the red and black lines in Fig. 5D. Positive values imply smaller output losses and a less severe recession. For example, a positive value of 0.05 on the y-axis corresponds to a 5 percent smaller reduction in cumulative output during the reopening phase.

The first set of headline results of the paper are given by Fig. 6, which traces out the large effects of virological testing on output losses and total deaths. The red dashed line in Panel A shows that virologically testing the population every week can reduce output losses by 25 percent and even 15 percent at a monthly frequency. Panel B shows that cumulative deaths are reduced by roughly 65 percent and 30 percent, respectively. At the other extreme, virologically testing the population quarterly reduces output losses by only 5 percent. Despite moderate output gains, the cumulative death rate is still reduced by 10 percent, corresponding to roughly 50,000 lives saved.

Serological tests are much less effective at mitigating output losses and reducing deaths. The dotted blue line traces out the effects of serological testing. Even with weekly testing, serological tests only reduce output losses and deaths by 6 percent during the reopening phase. The reduction in deaths corresponds to 30,000 lives saved; however at every testing frequency, virological tests strictly dominate serological tests in terms of outcomes.

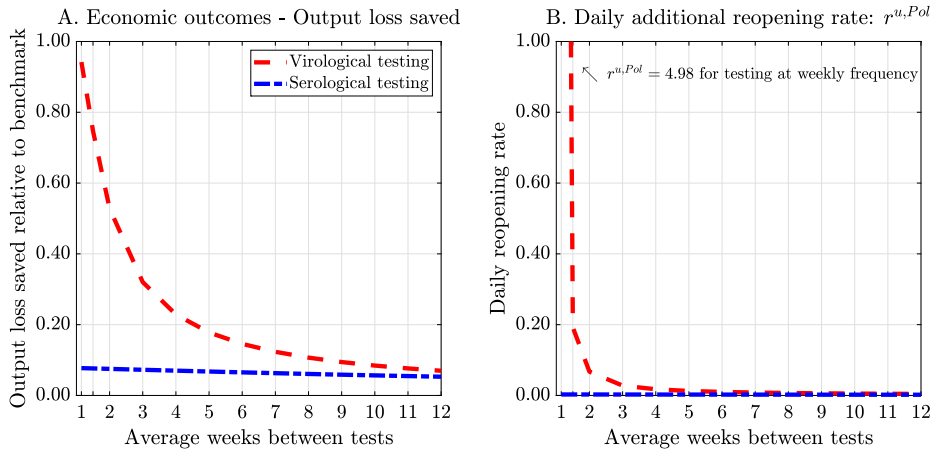
5.2. Testing with additional reopening:  $r^{u,Pol} > 0$

How much better economic outcomes could the US obtain if it suffered the same deaths it is currently on track to incur? To answer this question, we quantify the maximum possible savings in lost output that can be obtained with testing under an additional reopening policy that keeps deaths capped at the level of the benchmark model. The additional reopening policy slackens quarantine measures by setting  $r^{u,Pol}$  to a positive, fixed value. We then find the value of  $r^{u,Pol}$  such that



Notes: In this case  $\{r^{u,Pol} = 0\}$ , such that reopening policy is as in the benchmark calibration. Panel A. Output loss saved is computed as follows. During the reopening phase between June 1, 2020 and March 20, 2021 we compute total output loss relative to the non-Covid baseline—under which daily output is equal to 1 ( $Y_0 = 1$ )—and then divide by the same measure for the benchmark case in which there is only quarantine:  $\sum_d (1 - Y_d^{Testing}) / \sum_d (1 - Y_d^{Benchmark})$ . Panel B. Lives saved is computed as follows:  $(\sum_d D_d^{Benchmark} - \sum_d D_d^{WithTests}) / \sum_d D_d^{Benchmark}$ .

Fig. 6. Effects of testing without additional reopening: ( $r^{u,Pol} = 0$ ).



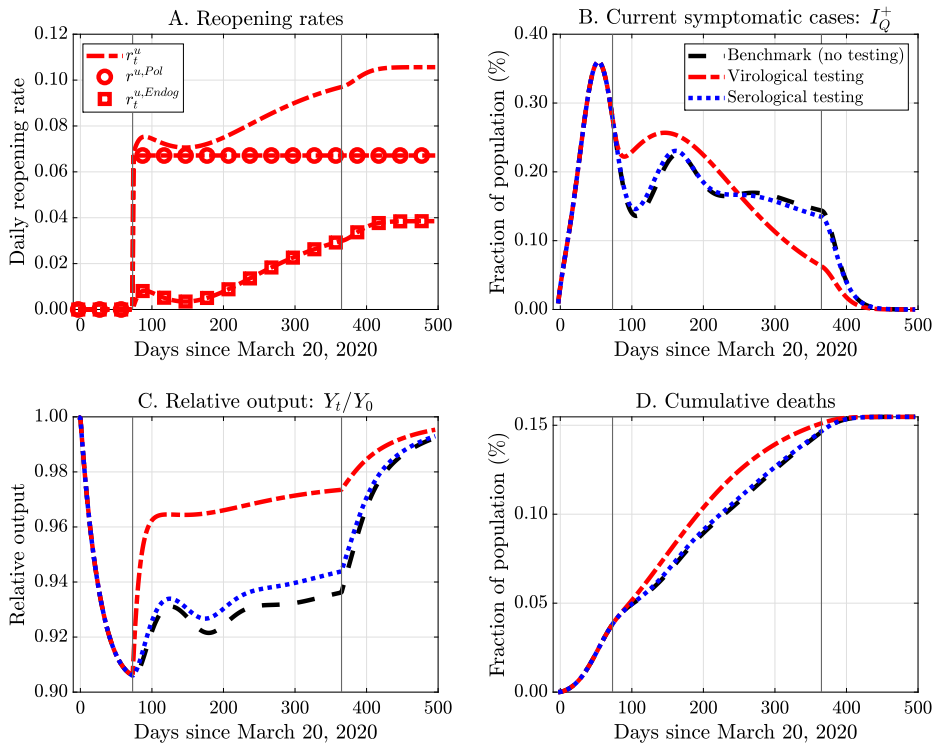
Notes: In this case  $r^{u,Pol} > 0$  is chosen to match long-run deaths as testing frequency varies along x-axis. The reopening rate  $r_t^u$  is expressed at a daily frequency. Panel A plots the output loss saved relative to the benchmark quarantine-only policy, see notes to Fig. 6A Panel B plots the value of  $r^{u,Pol}$  that generates constant long run deaths.

Fig. 7. Effects of testing under targeted quarantine policy - Constant long-run deaths.

deaths do not exceed the benchmark economy. We keep the same function form for  $r_t^u$  (6) such that the deaths due to the additional reopening will lead to changes in  $r_t^{u,Endog}$ .

Our main result is that potential output savings range from 95 down to 22 percent with weekly to monthly testing (Fig. 7A). Panel B plots the reopening rate policy  $r^{u,Pol}$  that leads deaths to be the same under the baseline. Since lives saved under the virological testing and only endogenous reopening were large (Fig. 6B), there is substantial slack in public health outcomes to be used up by additional reopening. The small degree of slack generated by serological testing means that even a small amount of reopening increases deaths above the benchmark level, hence output loss saved is only slightly larger than in Fig. 6A.

To visualize the implications for the progress of the pandemic and output, Fig. 8 replicates Fig. 5 under additional reopening. Panel D verifies that long-run deaths are the same in the benchmark no-testing regime versus the regime with both virological tests and additional reopening. We plot the two components of reopening in Panel A: the exogenous additional reopening  $r_t^{u,Pol}$ , and the endogenous reopening  $r_t^{u,Endog}$ . The total reopening rate  $r_t^u$  is the sum of these two components. Early on, the exogenous policy component accounts for most of the total reopening rate. The abrupt increase in reopening causes deaths, which initially suppresses the endogenous reopening component. Later on, as the virological testing regime begins to lower deaths, the endogenous reopening rate increases. Increased testing lowers deaths enough that individuals endogenously exit quarantine. Thus testing combined with more aggressive reopening policy generates a sharp rebound in



Notes: Panel A decomposes the reopening rate  $r_t^u$  into the constant policy piece  $r_t^{u,Pol}$  and the time-varying endogenous piece  $r_t^{u,Endog}$  according to (6).

Fig. 8. Testing every two weeks and additional reopening  $r_t^{u,Pol} > 0$  with constant long-run deaths.

output, with the level of output being half as low as under the benchmark. As now expected, the effects of the serological tests are minor.

In summary, we find that a targeted quarantine policy along with virological testing can accommodate an aggressive reopening policy that has the scope for significantly better economic outcomes and no worse health outcomes. We now turn to implementation of virological testing given these results.

## 6. Test quality vs. quantity

In implementing virological testing, we consider a simple counterfactual that shows that a planner would be willing to trade-off test quality for test frequency.<sup>29</sup> We have shown that the effects of virological testing on public health outcomes are highly non-linear (Fig. 7B). In particular, testing and quarantining at much higher frequencies sharply reduce deaths. Suppose that there were a quantity/quality trade-off such that, given a testing budget, better, more expensive tests could be administered infrequently, or poorer, cheaper tests administered frequently. The non-linearity suggests a planner may be willing to bear significantly poorer quality. This is a recent policy considered by the FDA, which on July 29, 2020 issued guidance for *At-Home* testing.<sup>30,31</sup>

We compare two virological tests which we view as representing the standard Polymerase Chain Reaction (PCR) test, and an alternative we call an *At Home Test* (AH test). These tests differ in two dimensions. First, the PCR test has a zero percent false negative rate—consistent with our analysis so far—, while the AH test has extremely poor sensitivity, yielding a 50 percent false negative rate. This is substantially worse than usual FDA requirements of a false negative rate of less than 20 percent. An individual in state (*TA*) or (*PA*) and *unknown* that receives a false negative simply remains *unknown*. Second, we assume that the cost of the tests scales linearly: the PCR test which we consider being administered monthly costs \$40 per test, and the AH test which we consider being administered weekly costs \$10 per test.<sup>32</sup> Both regimes therefore have the same monthly cost which we view as a useful benchmark. They also have the same specificity: a false positive rate of zero.

<sup>29</sup> For a contemporaneous analysis with similar results see the following working paper: Larremore et al. (2020).

<sup>30</sup> <https://www.fda.gov/news-events/press-announcements/coronavirus-covid-19-update-fda-posts-new-template-home-and-over-counter-diagnostic-tests-use-non>.

<sup>31</sup> For a contemporaneous analysis, see Larremore et al. (2020).

<sup>32</sup> This is the test-price that can be charged to Medicare by contractors <https://www.cms.gov/files/document/mac-covid-19-test-pricing.pdf>.

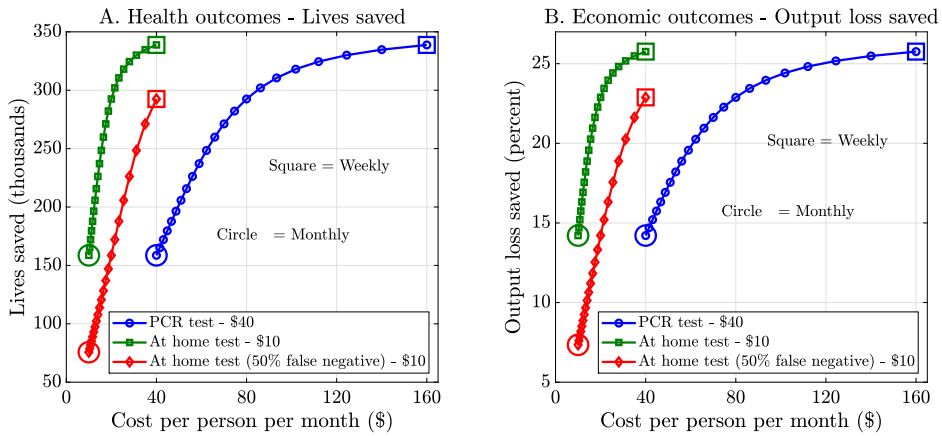


Fig. 9. More frequent testing with poorer quality tests dominates in terms of both public health and economic outcomes.

Our main result is that even with such poor sensitivity, weekly testing dominates: more lives are saved and output losses are lower, at a lower cost. Fig. 9 presents a simple cost-benefit analysis. In blue circles and red diamonds we compare the two tests. Panel A shows that at a cost of \$40 per month per person, the less sensitive AH test delivers a saving of around 300,000 lives. To save the same number of lives relative to the benchmark with the PCR test, testing would need to be at least every two weeks and cost more than \$80 per month per person. By lowering deaths by more, the weekly AH test leads to an increase in reopening, which reduces output losses. Panel B shows that at a cost of \$40 per month per person, the less sensitive test leads to reopening that reduces output losses by 23 percent, while at the same cost the PCR test leads to only an 14 percent dampening. As we have shown, additional reopening could use the lives saved to reduce output losses by even more for the AH test.

This simple exercise shows that the extreme non-linearities that occur due to testing and targeted quarantine at higher frequencies have important consequences for policy trade-offs across testing regimes. Importantly, the FDA could approve cheaper tests with very high false negative rates and achieve lower healthcare costs, better healthcare outcomes and better economic outcomes.

### 7. Robustness

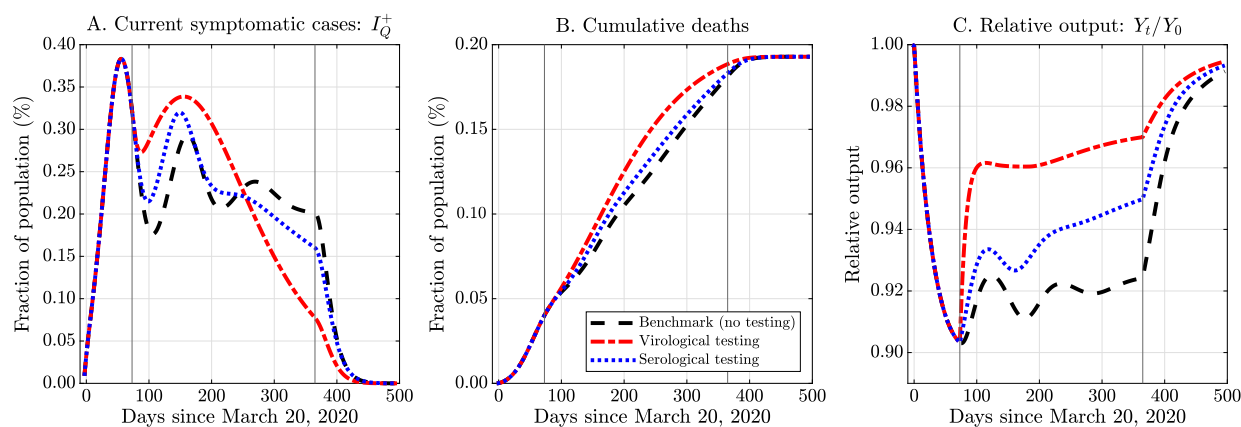
We show robustness of our quantitative conclusions regarding serological and virological testing with respect to a substantive model assumption. In the appendix we show robustness with respect to parameters and target moments.

*Immunity passports.* Throughout we have assumed that symptomatic individuals transition to the *known negative* information state. This assumption may be strong. Without a test verifying that they have previously contracted Covid-19 the government may be unwilling to lift their quarantine. This potentially biases results against serological testing.

Qualitatively we show that this is the case, but the effects are quantitatively small. To make this point clearly we go one step further and make virological tests irrelevant for the information state of a recovered individual. Regardless of past symptoms and virological tests, we assume an individual must receive a serological test before being granted an ‘immunity passport’ and being released. That is, known cases of infected-symptomatic ( $I_Q^+$ ) and permanently-asymptomatic ( $PA_Q^+$ ), now transition to recovered-unknown ( $R_Q^u$ ).

Fig. 10C shows that our conclusions with respect to the effectiveness of tests remain qualitatively and quantitatively similar to our main counterfactual (Fig. 8). Baseline deaths are higher as recovered negative cases no longer circulate. But when we compare output losses across counterfactuals that keep long-run deaths constant, we effectively control for this. Serological tests now permit wider reopening and a smaller drop in output but, again, these effects are small. Virological tests are now less powerful as they no longer grant immunity passports to those that were tested while asymptomatic; these effects are also small. We conclude that the main results of our benchmark exercise are not due to (i) symptomatic infection conveying future recovery, nor (ii) the double-duty of the virological test in identifying current infected *and* future recovered cases.

*Parameters and moments.* In the appendix we show how reopening varies under the two testing regimes as we vary targets and parameters. In all cases we recalibrate  $\rho^S$  and  $\omega^D$  such that the model matches the same empirical  $R_0^C$  and infection fatality rate, and then conducts the same ‘constant deaths’ counterfactual. We show that this benchmarking is key for understanding comparative statics. First, changes in the target IFR have no effect on the amount of output losses mitigated through testing, conditional on matching  $R_0^C$ . Second, under a lower  $\rho^A < \rho^S$ , lower  $R_0^C$ , higher  $\psi$  (i.e. less permanently asymptomatic types), output saved through testing is *higher*. Third, when incubation and infection periods are longer, testing is also more effective in creating capacity for reopening. Online Appendix Section A contains full details and discussion of these exercises.



Notes: Panel A plots infections, Panel B plots cumulative deaths, and Panel C plots contemporaneous output losses.

Fig. 10. Robustness: Immunity passports require serological testing.

Table 3

Current testing at some universities - ranked by daily tests.

University	Period	Days	Tests	Daily tests	% tested <sup>1</sup>	State	% of state tests
<b>A. Current testing</b>							
U. Illinois – Urbana-Champaign	Aug 16–Oct 20	66	568,368	8,612	1031.4	IL	16.0
Cornell University	Aug 10–Oct 01	53	155,700	2,938	568.7	NY	3.6
Harvard University	Oct 14–Oct 20	7	17,171	2,453	59.9	MA	3.8
Massachusetts Institute of Technology	Aug 16–Oct 21	67	133,596	1,994	939.5	MA	3.8
Duke University	Aug 15–Oct 16	63	96,430	1,531	507.8	NC	5.8
Yale University	Oct 14–Oct 20	7	10,221	1,460	66.0	NY	7.1
University of Massachusetts Amherst	Aug 06–Oct 20	76	100,988	1,329	282.1	MA	2.8
Boston College	Aug 26–Oct 21	57	67,861	1,191	384.3	MA	2.1

Notes: Data from schools' websites. (1) The fraction of the total population of the university tested is an extreme lower bound for two reasons. First, we take data on college enrollment, and to compute total population assume a student/staff ratio of 4, which is the same as Yale University, one of the lowest in the US. Second, we assume that college enrollment is the same as in previous years, which also over-estimates the total on campus in August, 2020.

### 8. Discussion

We discuss two key departures of our model from US testing policy, and we show that these are not departures from policies in segments of the economy.

First, based on national testing data, one might conclude that the frequency of testing discussed in this paper is infeasible. As noted in Section 2, random testing at the highest rate observed in the US would lead to an individual being tested once every 11 months. We consider testing at frequencies from weekly to quarterly. Second, a key feature of the model is the testing of asymptomatic individuals. On August 24, 2020, the CDC reverted to earlier policy guidance of testing only when symptomatic or contact with a known case has occurred.<sup>33</sup> This paper quantifies the positive effects of counterfactual testing regimes. While it is not the role of this paper to understand the political economy of why low rates of testing were realized and why asymptomatic testing has not been a policy, however we can discuss whether high rates of testing asymptomatic individuals are feasible.

There are certain areas of the economy where testing is in fact more frequent than we considered in this paper, and asymptomatic individuals are regularly tested. Table 3 describes current, end of August 2020, testing at three colleges, and reopening strategies from a selection of schools.<sup>34</sup> Schools are planning on, and some are already executing, tests at a rate of twice per week for students living on campus. Relative to non-college testing these rates are high, with University of Illinois (Urbana-Champaign) accounting for nearly 20 percent of state-wide tests. Meanwhile, the NBA tests around 1,655 players and staff daily, which represents around 6 percent of total tests in Florida.

What accounts for these institutions being able to privately implement testing at high frequencies? First, private institutions internalize the dampening of revenue loss associated with testing and reopening which is the focus of this paper. Ideally these would be internalized by a policy making authority such as the government, but we are not in a position to discuss whether this was or was not the case in practice. Second, private institutions are free to choose their own testing rules. This has included the development of saliva based tests. These were approved by the FDA after their extensive use by

<sup>33</sup> See: <https://www.cdc.gov/coronavirus/2019-ncov/hcp/testing-overview.html>.

<sup>34</sup> These schools were chosen due to the availability of detailed, publicly available, plans.

the NBA and used at UIUC before FDA approval.<sup>35</sup> Third, private institutions have different tools for punishment including loss of employment. This would allow for better enforcement of quarantine after positive tests.

In summary, private institutions have managed to implement plans that have circumvented supposed bottle-necks in the health-care system. This provides evidence that there are, and have been for some time, available technologies and strategies for massively higher rates of testing. We assume there will be an on-going discussion as to why the testing regime in the US was so far inside this technological frontier.

## 9. Conclusion

This paper introduces testing and several other pertinent features into a standard SEIR model of infectious disease transmission, and shows that public health policies can be of first order importance for economic trade-offs. In particular, testing and reopening can slacken the output-mortality trade-off that is the feature of many economic models of the pandemic that consider only lockdown policies.

Quarantine policies can only depend on observed health states, which creates a role for testing in distinguishing between infected and non-infected asymptomatic individuals. Our model, calibrated to the US in March-August 2020, demonstrates that testing asymptomatic individuals can stand-in for economically costly quarantine measures. We make this notion precise by reopening the economy as we test such that the overall mortality rate of the pandemic remains constant. With fewer individuals quarantined, output of the economy would decline substantially less, with testing every two weeks halving the loss in output. Testing allows the government to do better in terms of both deaths and output.

Our analysis comes with two important caveats. First, we study an ex-ante homogeneous population. Despite this, our framework demonstrates that incomplete information, testing and targeted quarantine policies can be simply and intuitively integrated into a richer model. Second, we take a reduced form approach to the behavioral response of reopening to public health risks. This is as opposed to behavioral economic models that integrate epidemiology as in Kremer (1996), Greenwood et al. (2019), or more recently Jones et al. (2020), Brotherhood et al. (2020), Keppo et al. (2020), Toxvaerd (2020), and Farboodi et al. (2020). Our exercises show that adding incomplete information and a role for testing through targeted quarantine does not overly complicate the baseline model and allows discussion of testing policies that cannot be discussed in the baseline complete information model. As such this framework could be integrated into models that are richer in terms of both heterogeneity and economic behavior.

## Appendix A. Supplementary material

Supplementary material related to this article can be found online at <https://doi.org/10.1016/j.red.2020.11.003>.

## References

- Acemoglu, D., Chernozhukov, V., Werning, I., Whinston, M.D., 2020. Optimal Targeted Lockdowns in a Multi-Group SIR Model. Working Paper 27102. National Bureau of Economic Research.
- Alvarez, F.E., Argente, D., Lippi, F., 2020. A Simple Planning Problem for COVID-19 Lockdown. Working Paper 26981. National Bureau of Economic Research.
- Atkeson, A., 2020a. How Deadly Is Covid-19? Understanding the Difficulties with Estimation of Its Fatality Rate. NBER Working Paper 26965. National Bureau of Economic Research.
- Atkeson, A., 2020b. What Will Be the Economic Impact of COVID-19 in the US? Rough Estimates of Disease Scenarios. Working Paper 26867. National Bureau of Economic Research.
- Atkeson, A., Kopecky, K., Zha, T., 2020. Four Stylized Facts about COVID-19. Working Paper 27719. National Bureau of Economic Research.
- Brauer, F., Castillo-Chavez, C., 2012. Mathematical Models in Population Biology and Epidemiology. Texts in Applied Mathematics, vol. 2. Springer.
- Brotherhood, L., Kircher, P., Santos, C., Tertilt, M., 2020. An economic model of the Covid-19 epidemic: the importance of testing and age-specific policies.
- Byambasuren, O., Cardona, M., Bell, K., Clark, J., McLaws, M.-L., Glasziou, P., 2020. Estimating the extent of asymptomatic Covid-19 and its potential for community transmission: systematic review and meta-analysis. MedRxiv.
- Chowell, G., Fenimore, P., Castillo-Garsow, M., Castillo-Chavez, C., 2003. SARS outbreaks in Ontario, Hong Kong and Singapore: the role of diagnosis and isolation as a control mechanism. *Journal of Theoretical Biology* 224 (1), 1–8.
- Cori, A., Ferguson, N.M., Fraser, C., Cauchemez, S., 2013. A new framework and software to estimate time-varying reproduction numbers during epidemics. *American Journal of Epidemiology* 178 (9), 1505–1512.
- Eichenbaum, M.S., Rebelo, S., Trabandt, M., 2020. The Macroeconomics of Epidemics. Working Paper 26882. National Bureau of Economic Research.
- Farboodi, M., Jarosch, G., Shimer, R., 2020. Internal and External Effects of Social Distancing in a Pandemic. NBER Working Paper 27059. National Bureau of Economic Research.
- Feng, Z., 2007. Final and peak epidemic sizes for SEIR models with quarantine and isolation. *Mathematical Biosciences and Engineering* 4 (4), 675–686.
- Fenichel, E.P., 2013. Economic considerations for social distancing and behavioral based policies during an epidemic. *Journal of Health Economics* 32 (2).
- Fernández-Villaverde, J., Jones, C.I., 2020. Estimating and Simulating a SIRD Model of COVID-19 for Many Countries, States, and Cities. Working Paper 27128. National Bureau of Economic Research.
- Furukawa, N., Brooks, J., Sobel, J., 2020. Evidence supporting transmission of severe acute respiratory syndrome coronavirus 2 while presymptomatic or asymptomatic. *Emerging Infectious Diseases* 26 (7).
- Gatto, M., Bertuzzo, E., Mari, L., Miccoli, S., Carraro, L., Casagrandi, R., Rinaldo, A., 2020. Spread and dynamics of the COVID-19 epidemic in Italy: effects of emergency containment measures. *Proceedings of the National Academy of Sciences of the United States of America* 117 (19), 10484–10491.
- Glover, A., Heathcote, J., Krueger, D., Rios-Rull, J.-V., 2020. Health versus Wealth: On the Distributional Effects of Controlling a Pandemic. NBER Working Paper 27046. National Bureau of Economic Research.

<sup>35</sup> See <https://news.yale.edu/2020/08/15/yales-rapid-covid-19-saliva-test-receives-fda-emergency-use-authorization>.

- Greenwood, J., Kircher, P., Santos, C., Tertilt, M., 2019. An equilibrium model of the African HIV/AIDS epidemic. *Econometrica* 87 (4), 1081–1113.
- Kornstein, A., 2020. Social Distancing, Quarantine, Contact Tracing, and Testing: Implications of an Augmented SEIR-Model. Discussion paper. Federal Reserve Bank of Richmond.
- Hortaçsu, A., Liu, J., Schwiag, T., 2020. Estimating the Fraction of Unreported Infections in Epidemics with a Known Epicenter: an Application to COVID-19. NBER Working Paper 27028. National Bureau of Economic Research.
- Imperial College Covid-19 Response Team, T., 2020. Impact of non-pharmaceutical interventions (NPIs) to reduce COVID19 mortality and healthcare demand. Mimeo.
- Jones, C.J., Philippon, T., Venkateswaran, V., 2020. Optimal Mitigation Policies in a Pandemic: Social Distancing and Working from Home. Working Paper 26984. National Bureau of Economic Research.
- Kaplan, G., Moll, B., Violante, G., 2020. Pandemics according to HANK.
- Keppo, J., Quercioli, E., Kudlyak, M., Smith, L., Wilson, A., 2020. The Behavioral SIR Model, with Applications to the Swine Flu and COVID-19 Pandemics.
- Kimball, A., Hatfield, K.M., Arons, M., James, A., Taylor, J., Spicer, K., Bardossy, A.C., Oakley, L.P., Tanwar, S., Chisty, Z., et al., 2020. Asymptomatic and presymptomatic SARS-CoV-2 infections in residents of a long-term care skilled nursing facility—King County, Washington, March 2020. *Morbidity and Mortality Weekly Report* 69 (13), 377.
- Kremer, M., 1996. Integrating behavioral choice into epidemiological models of AIDS\*. *The Quarterly Journal of Economics* 111 (2), 549–573.
- Kucharski, A.J., Russell, T.W., Diamond, C., Liu, Y., Edmunds, J., Funk, S., Eggo, R.M., Sun, F., Jit, M., Munday, J.D., et al., 2020. Early dynamics of transmission and control of COVID-19: a mathematical modelling study. *Lancet. Infectious Diseases* 20 (5), 553–558.
- Larremore, D.B., Wilder, B., Lester, E., Shehata, S., Burke, J.M., Hay, J.A., Tambe, M., Mina, M.J., Parker, R., 2020. Test sensitivity is secondary to frequency and turnaround time for COVID-19 surveillance. <https://doi.org/10.1101/2020.06.22.20136309>, medRxiv.
- Li, Q., Guan, X., Wu, P., Wang, X., Zhou, L., Tong, Y., Ren, R., Leung, K.S., Lau, E.H., Wong, J.Y., Xing, X., Xiang, N., Wu, Y., Li, C., Chen, Q., Li, D., Liu, T., Zhao, J., Liu, M., Tu, W., Chen, C., Jin, L., Yang, R., Wang, Q., Zhou, S., Wang, R., Liu, H., Luo, Y., Liu, Y., Shao, G., Li, H., Tao, Z., Yang, Y., Deng, Z., Liu, B., Ma, Z., Zhang, Y., Shi, G., Lam, T.T., Wu, J.T., Gao, G.F., Cowling, B.J., Yang, B., Leung, G.M., Feng, Z., 2020. Early transmission dynamics in Wuhan, China, of novel coronavirus-infected pneumonia. *The New England Journal of Medicine* 382 (13), 1199–1207. PMID: 31995857.
- Ota, M., 2020. Will we see protection or reinfection in COVID-19? *Nature Reviews. Immunology* 20 (1), 1474–1741.
- Piguillem, F., Shi, L., 2020. The Optimal Covid-19 Quarantine and Testing Policies. Discussion paper. Einaudi Institute for Economics and Finance (EIEF).
- Stock, J.H., 2020. Data gaps and the policy response to the novel coronavirus. NBER Working Paper 26902. National Bureau of Economic Research.
- Toxvaerd, F., 2020. Equilibrium social distancing. *Cambridge Working Papers in Economics*.
- Wallinga, J., Teunis, P., 2004. Different epidemic curves for severe acute respiratory syndrome reveal similar impacts of control measures. *American Journal of Epidemiology* 160 (6), 509–516.
- Wang, C., Liu, L., Hao, X., Guo, H., Wang, Q., Huang, J., He, N., Yu, H., Lin, X., Pan, A., et al., 2020. Evolving Epidemiology and Impact of Non-pharmaceutical Interventions on the Outbreak of Coronavirus Disease 2019 in Wuhan, China. medRxiv.
- Wen, W., Su, W., Tang, H., Le, W., Zhang, X., Zheng, Y., Liu, X., Xie, L., Li, J., Ye, J., et al., 2020. Immune cell profiling of COVID-19 patients in the recovery stage by single-cell sequencing. *Cell Discovery* 6 (1), 1–18.
- World Health Organization, T., 2020. Report of the WHO-China Joint Mission on Coronavirus Disease 2019. Mimeo.
- Wu, J.T., Leung, K., Leung, G.M., 2020. Nowcasting and forecasting the potential domestic and international spread of the 2019-nCoV outbreak originating in Wuhan, China: a modelling study. *The Lancet* 395 (10225), 689–697.